Submitted to : *Geophysical Journal International*

Seismic waves in rocks with fluids and fractures

James G. Berryman[1,*]

[1]*University of California, Lawrence Berkeley National Laboratory,*

1 Cyclotron Road, MS 90R1116, Berkeley, CA 94720, USA

Abstract

Seismic wave propagation through the earth is often strongly affected by the presence of fractures. When these fractures are filled with fluids (oil, gas, water, CO_2, etc.), the type and state of the fluid (liquid or gas) can make a large difference in the response of the seismic waves. This paper summarizes recent work on methods of deconstructing the effects of fractures, and any fluids within these fractures, on seismic wave propagation as observed in reflection seismic data. One method explored here is Thomsen's weak anisotropy approximation for wave moveout (since fractures often induce elastic anisotropy due to nonuniform crack-orientation statistics). Another method makes use of some very convenient fracture parameters introduced previously that permit a relatively simple deconstruction of the elastic and wave propagation behavior in terms of a small number of fracture parameters (whenever this is appropriate, as is certainly the case for small crack densities). Then, the quantitative effects of fluids on these crack-influence parameters are shown to be directly related to Skempton's coefficient B of undrained poroelasticity (where B typically ranges from 0 to 1). In particular, the rigorous result obtained for the low crack density limit is that the crack-influence parameters are multiplied by a factor $(1 - B)$ for undrained systems. It is also shown how fracture anisotropy affects Rayleigh wave speed, and how measured Rayleigh wave speeds can be used to infer shear wave speed of the fractured medium. Higher crack density results are also presented by incorporating recent simulation data on such cracked systems.

*JGBerryman@LBL.GOV

1 INTRODUCTION

Fractures can play a key role in hydrology and in many oil and gas reservoirs. Small scale cracks and/or large scale fractures generally increase rock compliance (reduce stiffness), and thus lower seismic wave speeds. If the distribution in space and/or orientation of fractures present is not uniform and isotropic, then significant anisotropy can be observed in seismic data. Aligned vertical fractures are particularly important as they can lead to azimuthal dependence (Crampin, 1989; Winterstein, 1990) (*i.e.*, so that results depend on the direction in which any linear surface seismic array has been emplaced). Fracture-induced mechanical and/or wave propagation effects are also sensitive to fluids within the fractures. In particular, gas or air will have little effect, while liquids in fractures can stiffen them so much that liquid-saturated fractures are nearly as stiff as the surrounding rock. For partially liquid-saturated cracks and fractures, the fracture will be almost as compliant as a gas-filled fracture until 90 to 95% or more of the fracture volume is filled with liquid. Fractures having a distribution of patchy saturation (separate and distinct pockets of gas and liquid) [see White (1979), Berryman *et al.* (1988), Endres & Knight (1989), Mavko & Nolen-Hoeksema (1994), Dvorkin & Nur (1998), Johnson (2001), Berryman *et al.* (2002a), Berryman (2004)] can also behave differently from any of the other cases mentioned.

Fluids such as oil, gas, water, or CO_2 are typically involved in many of the problems of most practical interest. Resolution of various practical and scientific issues in the earth sciences (Wawersik *et al.*, 2001) depends on knowledge of fluid properties underground, and also how the fluids move (*i.e.*, migrate or oscillate). In environmental cleanup applications, the contaminants to be removed from the earth are typically liquids such as gasoline or oil, or ground water contaminated with traces of harmful chemicals. In commercial oil and gas

exploration, the fluids of interest are hydrocarbons in liquid or gaseous form. In analysis of the earth structure, partially melted rock is key to determining temperature and local changes of structure in the Earth's mantle (Berryman, 2000). In all these cases, the tool most commonly used to analyze the fluid content remotely is measurements of seismic (compressional and/or shear) wave velocities and amplitude changes at reflecting boundaries in the earth. Depending on the application, sources of these waves may be naturally occurring such as earthquakes, or man-made such as reflection seismic surveys at the surface of the earth, or ship-based survey methods over the ocean, vertical seismic profiling from boreholes to surface, or still more direct (but higher frequency) measurements using logging tools in either shallow or deep boreholes.

In many of the cases mentioned, a variety of possible explanations for the observed wave velocity and attenuation discrepancies between theory and experiment have been put forward, including viscoelastic effects (wave amplitude decrease due to frequency-dependent attenuation), fluid-enhanced softening of intragranular cementing materials, chemical changes in wet clays that alter mechanical properties, etc. Providing some of the analytical and computational tools needed for treating these difficult problems as well as others for various applications is one of the goals of the present work.

A review article by Berryman (1995) summarized the state of the art in effective medium theories as applied to isotropic, but nevertheless heterogeneous, rocks and rock/fluid mixtures. It will be assumed throughout this presentation that this review material is available and known to the reader and, therefore, no effort to recapitulate the AGU Handbook material will be made here. [Also, see Appendix C of Berryman & Grechka (2006) for a review focused specifically on EMT's for fractured/cracked media.] Then, we may concentrate on more recent developments that are the subject of the paper.

Section 2 briefly reviews the prior work on fractures in rock and introduces the Sayers & Kachanov (1991) crack-influence parameter approach. Section 3 shows one means by which the Sayers & Kachanov (1991) method can be reconciled with Gassmann's (1951) results for undrained fluid mechanical effects in anisotropic porous media, and in particular provides a quick derivation of the Mavko & Jizba (1991) result relating shear dependence on fluid modulus to the corresponding bulk dependence for low crack densities. Section 4 shows how the low crack density results can be used to deconstruct the crack density value ρ_c from field data. Examples showing the complementary influence of vertical cracks versus horizontal cracks on seismic velocities are presented for cases of low crack density media. Section 5 revisits the deconstruction analysis for the case of higher crack densities, making use of recent computer-based empirical results for the crack-influence parameters as deduced from simulation data (Berryman and Grechka, 2006). Section 6 summarizes the overall conclusions of the paper. Appendix A gives an overview of the crack-influence decomposition method (Sayers & Kachanov, 1991) as needed for the higher crack density regime. Appendix B presents the results for Thomsen's δ parameter (the most complicated one of the three) at higher crack densities. Appendix C collects the exact formulas for wave propagation through vertically transversely isotropic (VTI) media. Examples in this paper are limited to VTI cases, but the methods for fracture analysis are not themselves limited in any way by the symmetry.

2 ANISOTROPY DUE TO FRACTURES

Much of the prior work on effective medium theory (Berryman, 1995) and double-porosity dual-permeability modeling (Berryman & Wang, 2000; Berryman & Pride, 2002a; Pride & Berryman, 2003a,b) has involved calculations of isotropic effective properties. In almost all

cases, it is much harder to estimate anisotropic effective properties reliably because the first step in such a calculation requires knowledge of both the effects of an oriented and/or anisotropic inclusion, and prior knowledge of a distribution (both in spatial location and in orientation) of such inclusions. Then an additional calculation of the overall properties based on the microdistribution information is needed. Unfortunately, geophysicists seldom know the microdistribution of such inclusions, and so we are immediately handicapped in what we can do scientifically, along these lines, in most cases.

However, there is one notable exception, which is the case of flat cracks in otherwise homogeneous elastic media. This problem was originally studied in some detail by O'Connell & Budiansky (1974, 1977) and Budiansky & O'Connell (1976) They showed in particular that, in the flat crack limit, a single parameter — the crack density ρ_c — was sufficient to describe the behavior for isotropic systems. This analysis was good for representing the behavior at very low crack densities. In order to arrive at higher crack densities, these authors made use of an older effective medium theory sometimes called "self-consistent," and sometimes more accurately described as "asymmetric self-consistent." This approach had the drawback that it overpredicted the effect of cracks in reducing elastic compliance, and therefore gave a relatively low value $\rho_c \simeq 9/16 \simeq 0.56$ at which the cracked medium would fail (Bruner, 1976). But, since it is known that failure does not usually occur at such small crack densities, these overall predictions are often criticized on this basis. [See Henyey & Pomphrey (1982) and Zimmerman (1991) Hudson (1980, 1994) used a different method for the crack problem, *i.e.*, the so-called "method of smoothing" first introduced in the mathematics literature by Keller (1964). Keeping density corrections just to first order in the Hudson approach gives an improvement over the previously mentioned scheme. Hudson also introduced a second order correction (Hudson, 1986), but Sayers & Kachanov

(1991) point out that, for higher concentrations of cracks, this approach can violate Hashin & Shtrikman (1963) upper bounds on the moduli for this problem. They recommend instead using a differential scheme [also see Zimmerman (1991) for an excellent review of the DS applied to cracked media], because the DS results track Hudson's first order model at low concentration of cracks, but for isotropic systems they never violate the HS bounds at the higher concentrations.

2.1 Elastic energy and the crack density tensor

Sayers & Kachanov (1991) also introduce a very interesting and useful scheme in the paper mentioned previously, permitting the calculation of constants for anisotropic cracked media from estimates of the behavior (like that predicted by the DS) for the isotropic case. This approach is a tremendous simplification of an otherwise very difficult technical problem. The key idea they use is to introduce an elastic potential energy quadratic in the stress tensor (Kachanov, 1980) that can be expressed in terms of invariants of the stress tensor in various combinations involving the "crack density tensor." This method results in a fairly complicated energy potential function involving nine distinct terms, seven of which characterize the influence of a dense crack distribution on the elastic medium. But this function has the advantage that, upon linearization in the crack density, it reduces to only four terms. Two of these terms are the standard ones for the pure (uncracked) medium and the remaining two terms contain the linear contributions (increases in compliance) due to the cracks. Now it is also not obvious that linearization is permissible in all the crack density ranges of interest, but Sayers & Kachanov (1995) showed in later work that the remaining contributions from the fourth rank crack-density tensor are often small — and therefore negligible in many situations of practical interest. The neglect of these terms nevertheless

implies a certain amount of error in any calculation made based on their neglect. But — if this error is of the size of our measurement error or less — it should not be a serious impediment to studies and analysis of these systems. Appendix A summarizes the full Sayers & Kachanov (1991) scheme as it will be used in the remainder of this paper.

To give one example, we find that the first order corrections to the compliance matrix S_{ij} due to the presence of a low crack density ρ_c and an isotropic crack distribution take the form:

$$\Delta S_{ij}^{(1)} = \rho_c \begin{pmatrix} 2(\eta_1+\eta_2)/3 & 2\eta_1/3 & 2\eta_1/3 & & & \\ 2\eta_1/3 & 2(\eta_1+\eta_2)/3 & 2\eta_1/3 & & & \\ 2\eta_1/3 & 2\eta_1/3 & 2(\eta_1+\eta_2)/3 & & & \\ & & & 4\eta_2/3 & & \\ & & & & 4\eta_2/3 & \\ & & & & & 4\eta_2/3 \end{pmatrix}, \qquad (1)$$

where η_1 and η_2 are the two coefficients appearing at first order in ρ_c of the Sayers & Kachanov (1991) theory that depend on the presence of cracks, and $\rho_c = Nb^3/V$ is the crack density (here N/V is the number density and b is the radius of the flat cracks when they are penny-shaped as assumed here). These two coefficients can be determined for any crack density by computing the analytical form of the bulk and shear moduli from the compliance matrix $S_{ij}^* = S_{ij} + \Delta S_{ij}$ and then comparing the results one-to-one with the results from any effective medium theory one trusts. For these purposes, the differential scheme (DS) is the one that Sayers & Kachanov (1991) recommend, but the author has shown elsewhere that another scheme — a symmetric self-consistent scheme that is sometimes called the CPA (for coherent potential approximation) – gives very comparable results. These results can also be compared to rigorous bounds [see Berryman & Grechka (2006)] and, therefore, may be

used to obtain rigorous upper bounds on both $|\eta_1|$ and η_2. In the published studies of this type, it was determined that the value of $|\eta_1|$ is generally much smaller in magnitude than η_2. In particular, $|\eta_1/\eta_2| \leq 0.01$ is typical of the observed results for both DS and CPA. This approach will be explained more fully later in the present paper.

The real advantage of this approach can now be demonstrated very simply using a couple of examples. [Also, see Schoenberg & Sayers (1995) for another different, but nevertheless similar, point of view.]

First, consider the situation in which all the cracks in the system have the same vertical (z-)axis of symmetry. Then, the cracked/fractured system is not isotropic, and we have the first-order compliance correction matrix for horizontal fractures is:

$$\Delta S_{ij}^{(1)} = \rho_c \begin{pmatrix} 0 & 0 & \eta_1 & & & \\ 0 & 0 & \eta_1 & & & \\ \eta_1 & \eta_1 & 2(\eta_1+\eta_2) & & & \\ & & & 2\eta_2 & & \\ & & & & 2\eta_2 & \\ & & & & & 0 \end{pmatrix} . \tag{2}$$

Now it is also not difficult to see that, if the cracks were oriented instead so that all their normals were pointed horizontally along the x-axis, then we have one permutation of this matrix and, if instead they were all pointed horizontally along the y-axis, then we have a third permutation of the matrix. If we then want to understand the isotropic correction matrix in (1), we can just average these three permutations: *i.e.*, simply add the three ΔS's together and then divide by three. Having done that, we exactly recover the isotropic compliance corrections matrix displayed in (1). [Note that this method of averaging, although correct for contributions linear in ρ_c, does not necessarily work for corrections higher order in ρ_c.]

This construction shows in part both the power and the simplicity of the Sayers & Kachanov (1991) approach.

Next, consider the case when all cracks have their normals lying randomly in parallel planes. Then, if the parallel planes are taken to be horizontal, the cracks are all vertically aligned as in Figure 1. So, we immediately find the anisotropic (*i.e.*, vertical transverse isotropy or VTI) result valid to first order in ρ_c for randomly oriented vertical fractures:

$$\Delta S_{ij}^{(1)} = \rho_c \begin{pmatrix} (\eta_1+\eta_2) & \eta_1 & \eta_1/2 & & & \\ \eta_1 & (\eta_1+\eta_2) & \eta_1/2 & & & \\ \eta_1/2 & \eta_1/2 & 0 & & & \\ & & & \eta_2 & & \\ & & & & \eta_2 & \\ & & & & & 2\eta_2 \end{pmatrix}. \tag{3}$$

This same basic concept then works very well for any assumed symmetry that we might like to model. There is no additional work to be done when: (*i*) the isotropic results are known (for some effective medium theory, or EMT) and (*ii*) the layout of the two η's in the correction matrix ΔS have been determined once and for all for a given elastic symmetry resulting from a specific choice of crack orientation distribution. Sayers & Kachanov (1991) give a precise prescription for doing this. Although we make use of this prescription here, we will not show the details in order to avoid some of the mathematical complications inherent in their tensorial expressions.

There are interesting and important questions of uniqueness related to the inverse problem (*i.e.*, deducing the η's from seismic wave observations) since more than one type of distribution can give rise, for example, to vertical transverse isotropy (VTI). Then, the question is whether quantities such as the Thomsen parameters (Thomsen, 1986) of anisotropy can help

us to remove some of these possible ambiguities from the interpretations of field measurements. We have found, for example, that vertical and horizontal cracks produce Thomsen parameters with opposite signs, as we now show.

2.2 Thomsen parameters for vertical fractures

If we know the compliance correction matrix ΔS_{ij}, then we can quickly find expressions for the Thomsen seismic wave parameters for weak anisotropy [see Thomsen (1986; 1995; 2002), Rathore *et al.* (1995), Rüger (1998; 2002), Grechka (2005)]. Clearly, a weak anisotropy assumption (and when the anisotropy is truly due to cracks) will also be consistent with the small crack density assumption that was needed above to justify the use of the Sayers & Kachanov (1991) method together with the simple averaging approach.

There are three Thomsen parameters: γ, ϵ, and δ. Parameter γ is essentially the fractional difference between the SH-wave velocities squared in the horizontal and vertical directions for a VTI medium. Similarly, parameter ϵ is essentially the difference between the P-wave velocities squared in the horizontal and vertical directions. Parameter δ is more difficult to interpret, but contributes in an essential way both to near vertical P-wave speed variations, and also to the angular dependence of the SV-wave speed. There are a great many steps that go into Thomsen parameter calculations since the crack density effects are most conveniently expressed in terms of the compliance matrix while the Thomsen parameters are usually defined instead in terms of the stiffness matrix (inverse of the compliance matrix). The steps in this work will not be shown here, as they are all relatively straightforward. The final result is merely quoted for the case of randomly oriented vertical fractures considered in the previous subsection.

For present purposes, we want to show quickly just how this method works. So we will

concentrate on the two parameters easiest to understand, which are γ and ϵ. For these two parameters, we have the following results for vertical fractures:

$$\gamma_v = \frac{c_{66} - c_{44}}{2c_{44}} = -\rho_c \eta_2 \frac{E_0}{4(1+\nu_0)} = -\rho_c \eta_2 \frac{G_0}{2}, \tag{4}$$

and

$$\epsilon_v = \frac{c_{11} - c_{33}}{2c_{33}} = -\rho_c[(1+\nu_0)\eta_1 + \eta_2]\frac{E_0}{2(1-\nu_0^2)} \simeq -\frac{\rho_c \eta_2 G_0}{1-\nu_0}, \tag{5}$$

where $\nu_0 = (K_0 - 2G_0/3)/2(K_0 + G_0/3)$ is Poisson's ratio, and Young's modulus E_0 is related to the isotropic host medium's bulk (K_0) and shear (G_0) moduli by $1/E_0 = 1/9K_0 + 1/3G_0$, and $G_0 = E_0/2(1+\nu_0)$. In the final expression of (5), we have neglected the term proportional to $\eta_1 \rho_c$, as this term is normally very small (on the order of 1% of the term retained). It can also be shown that, for this model, the remaining Thomsen parameter δ takes exactly the same value as ϵ to lowest order in the crack density parameter.

Examples of Thomsen's parameters for various choices of effective medium theory (EMT) are displayed in Figure 2. The results illustrate how estimates of η_1 and η_2 obtained from four different isotropic estimation schemes [noninteracting or NI (Zimmerman, 1991), DS (Zimmerman, 1991), CPA (Berryman, 1980), and nonsymmetric self-consistent scheme of O'Connell & Budiansky (1974) or Budiansky & O'Connell (1976)] can then be used to predict what values Thomsen's parameters should take in field data.

Some judgment is required then as to the most appropriate EMT to use, and prior work shows that some knowledge of microstructure can serve as a very useful guide when making this choice [see Berge *et al.* (1993, 1995)]. But, for applications to cracked media, we find the NI method is good for low crack density and the DS method is a good choice for higher ρ_c.

2.3 Rayleigh wave speed

Now, to provide one relatively simple illustration of the use of what has been presented so far, consider the well-known formula for the Rayleigh wave speed $v = v_R$ in an isotropic medium [see Love (1927), Ewing *et al.* (1957), Al-Husseini *et al.* (1981), Weertman (1996)]:

$$\beta_S \beta_P = \beta_{2S}^4, \tag{6}$$

where $\beta_S = \sqrt{1 - v^2/v_s^2}$, $\beta_P = \sqrt{1 - v^2/v_p^2}$, $\beta_{2S} = \sqrt{1 - v^2/2v_s^2}$, with v_s being the (isotropic) shear wave speed and v_p being the (isotropic) compressional wave speed in the host medium. For an anisotropic medium having the same transversely isotropic (VTI) symmetry considered here (*i.e.*, for the case of randomly oriented vertical cracks), Musgrave (1959) shows that the equivalent result for the Rayleigh wave speed $v = v_R$ in the plane perpendicular to the VTI axis of symmetry is determined by the cubic equation

$$R(q) \equiv \frac{q^3}{16} - \frac{q^2}{2} + \left(\frac{3}{2} - \frac{c_{66}}{c_{11}}\right) q + \left(\frac{c_{66}}{c_{11}} - 1\right) = 0, \tag{7}$$

where $q \equiv \rho_0 v^2 / c_{66}$ and ρ_0 is the mass density of the host medium (which is assumed to be the same as that of the pure material without cracks, since the cracks are very flat and are not introducing any significant amount of porosity). [Note: It is not difficult to check that (6) and (7) are equivalent when the elastic medium is isotropic.]

The Newton-Raphson iterative method (Hildebrand, 1956; Press *et al.*, 1988) for finding zeroes of expressions nonlinear in a parameter, or in this case zeroes of a polynomial, is very useful for solving the problem posed in (7). Furthermore, it can be used to generate a convenient analytical expression that may be used as a good starting point for the iteration scheme, or possibly to gain some physical intuition about the problem. The Newton-Raphson

scheme is stated as

$$q_{i+1} = q_i - \frac{R(q_i)}{R'(q_i)}, \tag{8}$$

where q_i is the most recent guess or iterate, and q_{i+1} is the next one in the sequence. One especially simple choice of first iterate q_0 is $q_0 = 1$. Then, $R(1) = 1/16$ and $R'(1) = 11/16 - v_s^2/v_p^2$, where we have used the fact that $c_{66}/c_{11} = v_s^2/v_p^2$. It follows then that

$$q_1 \simeq 1 - \frac{1}{11 - 16v_s^2/v_p^2}. \tag{9}$$

Using the definition of Poisson's ratio $\nu_0 = (K - 2G/3)/2(K - G/3)$ together with the approximations that $c_{11} \simeq K + 4G/3$ and $c_{66} = G$ in the uncracked host material, we find that (9) reduces to

$$q_1 \simeq \frac{2 + 6\nu_0}{3 + 5\nu_0}, \tag{10}$$

and since $q_1 \simeq v_R^2/v_s^2$ also holds, we obtain an approximate expression for the Rayleigh wave speed in terms of host Poisson ratio and the shear wave speed of the cracked medium:

$$v_R \simeq v_s\sqrt{\frac{2 + 6\nu_0}{3 + 5\nu_0}}, \tag{11}$$

This formula should be an excellent approximation for the low crack density limit under consideration. It can nevertheless be improved by further Newton-Raphson iterations in a numerical scheme.

From the definitions of the Thomsen parameters γ and ϵ, it is now straightforward to see that

$$c_{66} = c_{44}(1 + 2\gamma) \tag{12}$$

and

$$c_{11} = c_{33}(1 + 2\epsilon). \tag{13}$$

In terms of Sayers & Kachanov (1991) parameters, for vertical cracks the shear modulus $c_{44} = G_0/(1 + \rho_c \eta_2 G_0)$, while c_{33} is found by inverting $S_{ij} + \Delta S_{ij}$ for the 33 component of the stiffness matrix. So we can now readily compute the Rayleigh wave speed by solving the cubic equation (7). Some results of this type are displayed in Figure 3. In particular, we find that the crack density is indeed a good parameter to use, as all these plots for different choices of crack aspect ratio clearly overlap to numerical accuracy in the low crack density range, which is typically considered to be $0 \leq \rho_c \leq 0.1$.

2.4 Inverting for shear wave speed

Equation (7) for Rayleigh wave speed is normally used to compute v_R when shear wave speed $v_s = \sqrt{c_{66}/\rho_0}$, and compressional wave speed $v_c = \sqrt{c_{11}/\rho_0}$ are both known. But the same equation can be used instead to determine the shear wave speed v_s if instead the Rayleigh wave speed v_R and the compressional wave speed v_c are both known. This technique is important in practice because the Rayleigh wave is very easy to excite, and its amplitude decays slowly with distance from the source. In fact, in normal seismic reflection processing, the Rayleigh wave is easier to excite and observe than the compressional wave, and tends to mask the main seismic wave of most interest in the region nearest the seismic source. In soft surface materials and/or ocean sediments, it can also be very difficult to excite shear waves directly with surface sources. So the inversion approach suggested is a viable method of determining the shear wave speed. In fact, this method has been used on land by Jones (1958) and the corresponding method for ocean bottom acoustics (making use of the Stoneley wave, instead of the Rayleigh wave) has been used by Bucher *et al.* (1964), and by Berge *et al.* (1991) specifically for the anisotropic case. This simple version of the method is necessarily restricted to Rayleigh (Stoneley) waves over (*i.e.*, at the fluid-

solid interface of) an elastic medium, homogeneous at least to the depth of one Rayleigh (Stoneley) wavelength; a generalization for layered media is needed otherwise.

Thus, the formula shown previously in (7) is pertinent, but it needs to be used in a different way to find the shear wave speed $v_s = \sqrt{c_{66}/\rho_0}$, when $v_p = \sqrt{c_{11}/\rho_0}$ and v_R are known.

To accomplish this goal, we first square (6). The result is a quartic equation for $q = (v_R/v_s)^2$. In the situation now under consideration, v_R is known, but v_s is unknown (opposite of the earlier case). But this difference does not cause any difficulty in the analysis. The equation can be conveniently rearranged into the form:

$$R(q) \equiv \frac{q^4}{16} - \frac{q^3}{2} + \frac{3}{2}q^2 - \left(1 + \frac{v_R^2}{v_p^2}\right) q + \frac{v_R^2}{v_p^2} = 0. \tag{14}$$

Again, equation (14) is straightforward to solve by iteration using a simple Newton-Raphson scheme (Hildebrand, 1956; Press *et al.*, 1988). One good starting value for the scheme will often be $q \simeq 0.8$, as this corresponds roughly to a trial value of $v_R = 0.9 v_s$.

There is some analytical insight to be gained however by repeating the analysis of the previous subsection for this problem. Again, it is advantageous to consider the starting iterate $q_0 = 1$. Then, $R(1) = 1/16$, as before. But now $R'(1) = 3/4 - v_R^2/v_p^2$. Using (8), the result is that

$$q_1 \simeq 1 - \frac{1}{12 - 16 v_R^2/v_p^2}. \tag{15}$$

Since $q_1 \simeq v_R^2/v_s^2$, we then have

$$v_s \simeq v_R \sqrt{1 + (11 - 16 v_R^2/v_p^2)^{-1}}. \tag{16}$$

This formula works well as a first approximation to v_s, while (15) can be used as the starting estimate in a Newton-Raphson iteration scheme to obtain a better answer.

Having once determined the value of $v_s = \sqrt{c_{11}/\rho_0}$ — using the measured Rayleigh wave speed v_R and the compressional wave speed v_p — in the symmetry plane, Thomsen parameter analysis can be combined with the Sayers & Kachanov (1991) method in order to deduce useful information about the nature of the heterogeneities causing the anisotropic at the macroscale. Once these wave speeds are known, the analysis for interpretation can proceed in essentially the same manner as in the previous example.

3 GASSMANN'S EQUATIONS AND FRACTURED MEDIA

For applications to oil and gas reservoirs or hydrology, it is also important to make a connection between the fracture results quoted above and Gassmann's results (Gassmann, 1951; Brown & Korringa, 1975; Berryman, 1999) for fluid saturated and undrained porous media. Even very flat cracks might harbor some fluid at various times and the question is how this fluid affects the response of the cracks.

Recall first that Gassmann's result (Gassmann, 1951) on the effect of fluids in a porous medium, isotropic or anisotropic, can be expressed (in a manner similar to the preceding analysis for fractures) by using a compliance correction matrix of the form:

$$\Delta S_{ij} = -\gamma^{-1} \begin{pmatrix} \beta_1^2 & \beta_1\beta_2 & \beta_1\beta_3 & & & \\ \beta_1\beta_2 & \beta_2^2 & \beta_2\beta_3 & & & \\ \beta_1\beta_3 & \beta_2\beta_3 & \beta_3^2 & & & \\ & & & 0 & & \\ & & & & 0 & \\ & & & & & 0 \end{pmatrix}, \tag{17}$$

where effects of the fluid bulk modulus appear only in the factor γ, and the coefficients β_1,β_2,β_3 satisfy a sumrule of the form $\sum_{i=1}^{3} \beta_i = \alpha/K_d = 1/K_d - 1/K_m$, and $\alpha = 1 - K_d/K_m$

is the Biot-Willis coefficient (Biot & Willis, 1957). So, in the two simplest cases, we have: (1) $\beta_1 = \beta_2 = 0$, $\beta_3 = \alpha/K_d$ for the case of horizontal fractures, and (2) $\beta_1 = \beta_2 = \beta_3 = \alpha/3K_d$ for the case of an isotropic distribution of fractures. Other cases may be considered by introducing positive fractions x_1, x_2, x_3, where $x_i \leq 1$ for all i, and $\sum_i x_i \equiv 1$, so that $\beta_i = \alpha x_i/K_d$.

The bulk moduli K_d and K_m are, respectively, the drained (porous) bulk modulus of the overall system and the mineral modulus whenever there is only one mineral present in the system (as will be assumed here for the present analysis). [The scalar drained modulus K_d for an anisotropic system is identical to the Reuss average for the bulk modulus of the compliance matrix of the porous system. See Berryman (2004b).] When the system is responding anisotropically as in the case of a set of cracks having a vertical symmetry axis like example (2), it is appropriate to make (17) compatible with the structure of (2) by setting $\beta_1 = \beta_2 = 0$, so $\beta_3 = \alpha/K_d$. Although it is then tempting to treat the anisotropic probem by making an *ad hoc* fluid-dependent perturbation to $\eta_2\rho_c$ while ignoring $\eta_1\rho_c$, since its value is two orders of magnitude smaller, we will find that the full analysis is not very difficult. We show later in the section that the usual *ad hoc* corrections differ in some significant ways from the exact results obtained here.

3.1 Bulk modulus response

Recall that Gassmann's formula for an isotropic medium can be written in the form:

$$K_u = K_d + \frac{\alpha^2}{(\alpha - \phi)/K_m + \phi/K_f} = \frac{K_d}{1 - \alpha B}, \tag{18}$$

where K_u is the undrained bulk modulus, K_d is the drained bulk modulus, K_m is the mineral or solid modulus, K_f is the bulk modulus of the pore fluid, ϕ is the porosity and $\alpha =$

$1 - K_d/K_m$. The coefficient B is Skempton's coefficient (Skempton, 1954). The value of Skempton's coefficient B is determined by rearranging (18) in terms of compliances (instead of stiffnesses), as

$$\frac{1}{K_u} - \frac{1}{K_d} = -\frac{\alpha}{K_d}\left[1 + \frac{K_d\phi}{K_f\alpha}\left(1 - \frac{K_f}{K_m}\right)\right]^{-1} = -\frac{\alpha}{K_d}B. \tag{19}$$

Equation (19) thus serves as a definition of Skempton's coefficient B in terms of the other moduli of the system.

Now also recall that, for fractured media having no other porosity ϕ except the fractures themselves, we have

$$\phi = \frac{4\pi}{3}b^3\left(\frac{a}{b}\right)\frac{N}{V} = \frac{4\pi}{3}\left(\frac{a}{b}\right)\rho_c, \tag{20}$$

where the crack density is $\rho_c = Nb^3/V$, N/V is the number of cracks per unit volume, b is the radius of the (assumed) penny-shaped crack, and a/b is its aspect ratio. Assuming there is only one horizontal crack or a set of parallel horizontal cracks, we can make use of (2) since then the Reuss average of the bulk modulus of the drained cracked sample is given by

$$\frac{1}{K_d} = \frac{1}{K_m} + 2(3\eta_1 + \eta_2)\rho_c. \tag{21}$$

Equation (17), with $\beta_1 = \beta_2 = 0$, $\beta_3 = \alpha/K_d$, and $\gamma = \alpha/BK_d$, then implies that

$$\frac{1}{K_u} = \frac{1}{K_d} - \beta_3^2/\gamma = \frac{1 - \alpha B}{K_d}, \tag{22}$$

as expected. Furthermore, since

$$\frac{\alpha}{K_d} = \frac{1}{K_d} - \frac{1}{K_m} = 2(3\eta_1 + \eta_2)\rho_c \tag{23}$$

follows from (21), we also have from (22) and (23) that

$$\frac{1}{K_u} - \frac{1}{K_d} = -\frac{\alpha}{K_d}B = -2(3\eta_1 + \eta_2)\rho_c B. \tag{24}$$

Adding (23) to (24), we obtain

$$\frac{1}{K_u} - \frac{1}{K_m} = 2(3\eta_1 + \eta_2)\rho_c(1 - B). \tag{25}$$

So, the rigorous statement relating the Sayers & Kachanov parameters to the undrained modulus K_u is that all occurrences of η_1 and those occurrences of η_2 contributing to the part of the compliance matrix that operates on the principal stresses (σ_{11}, σ_{22}, σ_{33}) are all simply multiplied by a factor of $(1 - B)$, where B is Skempton's coefficient of undrained poroelasticity. This method is easily seen to be capable of treating consistently all the interesting cases of K_f from $K_f \simeq 0$ (having $B = 0$) to $K_f \simeq K_m$ (having $B = 1$). This method provides an interpolation scheme, but it is also a fully rigorous one, unlike the *ad hoc* schemes sometimes seen in the literature on this topic, which typically use a factor of $(1 - K_f/K_m)$ instead of the rigorous factor of $(1 - B)$.

To see how much difference there is between these two factors, we expand $(1 - B)$ and find

$$1 - B = \frac{1 - K_f/K_m}{1 - K_f/K_m + (K_f\alpha/\phi K_d)}. \tag{26}$$

From (23) and (20), we determine that the ratio

$$\frac{\alpha}{\phi K_d} = 3(3\eta_1 + \eta_2)/2\pi(a/b), \tag{27}$$

having cancelled out the factors of ρ_c. So the final term in the denominator of (26) is inversely proportional to the aspect ratio a/b. In the limit of small aspect ratios and finite values of $K_f \neq K_m$, we find that

$$1 - B \to O\left[a(1 - K_f/K_m)/b\right]. \tag{28}$$

Therefore, when the aspect ratio a/b becomes very small, we find that $1 - B$ goes to zero regardless of the value of K_f relative to K_m (as long as $K_f \neq 0.0$). This formula is physically

sensible because it provides a simple resolution to the possibly ambiguous situation in which the aspect ratio is extremely small, while we are uncertain about the presence or absence of fluid in the cracks. The formula says that, if the volume of the crack is negligible, then the effect of the finite fluid bulk modulus K_f is also negligible. This result is entirely reasonable, as K_f is a bulk property — not a surface property — and therefore should not be expected to influence bulk behavior due to very thin cracks in a macroscopic medium.

3.2 Shear modulus response

Now another interesting and important result is the Mavko & Jizba (1991) formula relating changes in fluid content induced in the bulk modulus to those induced in the shear modulus for very low crack density and isotropic media. For this calculation we can safely neglect the terms in η_1 as they are two orders of magnitude smaller than the already small contributions that we will be considering.

Again recall that the effective drained bulk (K_d) and shear (G_d) moduli are given by

$$\frac{1}{G_d} - \frac{1}{G_m} = \frac{4\eta_2\rho_c}{3} \tag{29}$$

and

$$\frac{1}{K_d} - \frac{1}{K_m} \simeq 2\eta_2\rho_c \tag{30}$$

[see equations (11) and (12) of Berryman and Grechka (2006)] for an isotropic system of randomly oriented cracks in host with moduli G_m and K_m.

The pertinent changes Δ_f to the undrained compliances due to the presence of a fluid bulk modulus differing from K_m (recall that $B = 1$ if $K_f = K_m$) in an isotropic system are therefore given [see Eq. (25)] by

$$\Delta_f\left(\frac{1}{K_u}\right) = 3\Delta_f(S_{11} + 2S_{12}) = -2\eta_2\rho_c\Delta_f(B) \tag{31}$$

for the undrained bulk modulus K_u. For the shear modulus in an isotropic system, we will have two contributions: First, for the principal stresses satisfying $\sigma_{11} = -\sigma_{22}$ we have:

$$\Delta_f \left(\frac{1}{G_{12}} \right) \equiv \Delta_f \left(2(S_{11} - S_{12}) \right) = -\frac{4}{3} \eta_2 \rho_c \Delta_f(B). \tag{32}$$

Then, the other shear contribution comes from the uniaxial shear modulus according to

$$\Delta_f \left(\frac{1}{G^r_{eff}} \right) = \Delta_f \left(2(S_{11} + S_{12} - 4S_{13} + 2S_{33})/3 \right) = -\frac{4}{3} \eta_2 \rho_c \Delta_f(B), \tag{33}$$

where G^r_{eff} has been defined previously [see Berryman (2004b) and Berryman(2006)] and is due in this instance to the presence of cracks saturated by the fluid. Note that these two shear contributions are numerically equal. Then, we easily recover the corresponding result of Mavko & Jizba (1991) by observing first that the total change in the undrained shear modulus for the isotropic system is

$$\Delta_f \left(\frac{1}{G_u} \right) = \frac{2}{5} \Delta_f \left(\frac{1}{G^r_{eff}} \right) + \frac{3}{5} \times 0, \tag{34}$$

since the three remaining contributions to shear compliance exhibit no fluid dependence and so do not contribute to (34). Finally, substituting (33) into (34) and then comparing to (31), we have

$$\Delta_f \left(\frac{1}{G_u} \right) = \frac{4}{15} \Delta_f \left(\frac{1}{K_u} \right), \tag{35}$$

in agreement with previous results of this type by Mavko & Jizba (1991) and Berryman *et al.* (2002). So this formalism provides an efficient means of correctly deriving both old and new results. Finally, recall that (35) is clearly an approximation, since we have neglected the terms proportional to $\eta_1 \rho_c$. The result must also be modified at high crack densities, but we will not pursue this possible generalization of the formula here.

Berryman *et al.* (2002) have also shown that the factor of $\frac{4}{15}$ in (35) holds strictly only for very flat cracks [consistent with the assumptions of Mavko & Jizba (1991)], and that the

appropriate factor in other situations can be either higher or lower than $\frac{4}{15}$, depending on details.

We expand on these and related topics using worked examples in the remaining sections of the paper.

4 DECONSTRUCTION FOR SMALL CRACK DENSITIES

The ultimate goal of the work presented has been to enable some approaches to the problem of characterizing reservoirs, especially reservoirs containing fractures, using seismic data. This idea is obviously not a new one (Bonner, 1974; Lynn *et al.*, 1995; Schoenberg & Sayers, 1995). But some of the consequences of the Sayers & Kachanov (1991) method need more detailed exploration and explication. We will provide some of that discussion in the following two examples: first treating a fairly typical reflection seismic example, and then showing how to use similar ideas in a different way for very shallow imaging and characterization.

4.1 Reflection seismic example for small ρ_c

Assume for the sake of argument that all three Thomsen parameters (Thomsen, 1986), γ, ϵ, and δ, have been determined for a given reservoir and that the reservoir exhibits VTI characteristics. [If the reservoir does not in fact exhibit VTI symmetry, then we might need to consider HTI (horizontal transverse isotropy) or some still more complicated type of anisotropy. [Such situations are not beyond these methods, but they are beyond our present scope.] For VTI, we need to know something about the variety of behaviors that are possible in the presence of fractures. Equations (4) and (5) show the results expected if the fractures

are vertical and randomly oriented. But there are obviously other possibilities as well, and to have a better chance of making a valid interpretation of the observed behavior, we need to know more about the range of possibilities for the Thomsen parameters. We will not try to be exhaustive here, but rather present one additional result that can clearly be distinguished by such data.

Consider first the case of horizontal fractures. Then, the axis of fracture symmetry is uniformly vertical, and so the reservoir would exhibit VTI symmetry again (just as in the case of vertical fractures randomly oriented). But the resulting expressions for the Thomsen parameters in terms of the Sayers & Kachanov (1991) parameters are quite different. We find for horizontal fractures that

$$\gamma_h = \frac{c_{66} - c_{44}}{2c_{44}} = \rho_c \eta_2 G_0, \tag{36}$$

and

$$\epsilon_h = \frac{c_{11} - c_{33}}{2c_{33}} = \rho_c[(1+\nu_0)\eta_1 + \eta_2]\frac{E_0}{(1-\nu_0^2)} \simeq \frac{2\rho_c \eta_2 G_0}{1-\nu_0}. \tag{37}$$

The background shear modulus is G_0, and the corresponding Poisson ratio is ν_0. Again, we find that $\delta = \epsilon$ to the lowest order in the crack density parameter. Also, we have neglected the term in η_1 in the final expression of (37), as this is on the order of a 1% correction to the term retained.

So we find that the magnitude of the coefficients in this case differs by a factor of 2 from those of randomly oriented vertical fractures as seen earlier in Eqs. (4) and (5). More importantly however, the sign of these expressions is *opposite* that for random vertical fractures. The factor of 2 and the sign difference are both easily understood in the context of Sayers & Kachanov (1991) parameters, because a certain average of these two results corresponds to an isotropic medium and, therefore, the Thomsen anisotropy parameters for these two cases

must average to zero in this case. [Recall that this statement's validity rests in part on the assumption of low crack densities ρ_c.] The appropriate average is twice the vertical fracture result added to the horizontal fracture result, and then this sum is divided by three. This method of construction gives equal weighting to each of the three component fracture sets, since the vertical fractures have only half of the total crack density ($\rho_c/2$) in the vertical example, whereas the horizontal fracture set has the full weight of ρ_c.

In both examples, the Thomsen parameter measurements may be used to estimate the magnitude of the $\rho_c\eta_2$ product assuming the background shear modulus G_0 and the background Poisson ratio ν_0 are either known, or can be accurately estimated. But, horizontally fractured systems can also be easily distinguished from vertically fractured systems, since the sign of the Thomsen coefficients is opposite in these two scenarios. These results are illustrated in Figures 4 and 5, using the same simulation examples as discussed previously from Berryman and Grechka (2006).

It would be helpful for interpretation purposes to enumerate other related scenarios that could be distinguished from these two by using the anisotropy parameter data. However, we will leave such problems — especially those involving azimuthal dependence (and therefore not VTI symmetry) — to future work. There is no fundamental problem with computing the relations between the Thomsen parameters and the Sayers & Kachanov (1991) parameters for arbitrarily complicated choices of fractured reservoir scenarios. All can be studied in a very straightforward way, but making good choices about which of the necessarily limited number of scenario that time permits us to consider and providing a general structure for the analysis are presumably two of the key steps in this process that require further study.

4.2 Shallow example for small ρ_c

The preceding example assumed that typical reflection seismic data collection could be performed at the site of interest. But suppose instead that the region of interest is quite shallow, possibly very soft and/or compliant sediments or soils, and that, in particular, it is not possible (either logistically or otherwise) to obtain shear wave data directly. Then what can be done?

One of the most common problems with traditional compressional wave surveys is ground roll. Ground roll is typically composed of Rayleigh and/or Love waves, and usually the Rayleigh wave component is the one we need to eliminate because it is contaminating the compressional wave data gathered near the shot point. As mentioned before, the Rayleigh wave speed depends on both the compressional and shear wave speeds of the medium, and – being a surface wave – it is most strongly influenced by the topmost layers of the earth (usually those within about one wavelength from the surface). So, for shallow imaging and analysis, why not consider using Rayleigh wave speed measurements together with P-wave speed measurements to infer the S-wave speed? The important S-wave speed in an anisotropic (VTI) medium is the shear wave speed in the symmetry plane (perpendicular to the axis of symmetry). Thus, the formula shown previously in (7) is still pertinent, but it needs to be used in a different way to find the shear wave speed $v_s = \sqrt{c_{66}/\rho_0}$, when $v_p = \sqrt{c_{11}/\rho_0}$ and v_R are known. We have already discussed this approach briefly in Section 2.4.

5 DECONSTRUCTION FOR LARGER CRACK DENSITIES

5.1 Second order corrections

For larger crack densities, we need to add higher order corrections into our analysis of the compliance corrections. The second order corrections in crack density for the case of horizontal fractures (having the vertical (z-)axis of symmetry again) are:

$$\Delta S_{ij}^{(2)} = \rho_c^2 \begin{pmatrix} 0 & 0 & & \eta_4 & & & \\ 0 & 0 & & \eta_4 & & & \\ \eta_4 & \eta_4 & 2(\eta_3+\eta_4+\eta_5) & & & & \\ & & & & 2\eta_5 & & \\ & & & & & 2\eta_5 & \\ & & & & & & 0 \end{pmatrix}. \tag{38}$$

Equation (38) is the second order correction corresponding to first order correction (2). The arguments of η_3, η_4, and η_5 are all understood to be zero. If (as is most likely to be the case) there are also higher order corrections to η_1 and η_2, then we should also relabel η_4 and η_5 as discussed in Appendix A, so that (for example, depending on available data) $\eta_4 \to \eta_4^v(0) \simeq \eta_4(0) + \eta_1'(0)$ and $\eta_5 \to \eta_5^v(0) \simeq \eta_5(0) + \eta_2'(0)$. The remaining contribution η_3 does not need shifting since it first appears at this order of the expansion in ρ_c.

Performing these various shifting tasks requires a great deal of information that will often not be available. Furthermore, it is not particularly useful information unless the goal is to characterize the system for all crack densities. We can characterize a given system well enough without performing any of these tasks, as long as terms in ρ_c^3 and higher order may be safely neglected (*e.g.*, for $\rho_c = 0.1$, terms of order $\rho_c^3 = 0.001$ are 1% of the first order corrections and 0.1% of the host contributions).

For completeness we note that the second order correction corresponding to the isotropic case is:

$$\Delta S_{ij}^{(2)} = \frac{2\rho_c^2}{3} \begin{pmatrix} (\eta_3+\eta_4+\eta_5) & (\eta_3+\eta_4) & (\eta_3+\eta_4) & & & \\ (\eta_3+\eta_4) & (\eta_3+\eta_4+\eta_5) & (\eta_3+\eta_4) & & & \\ (\eta_3+\eta_4) & (\eta_3+\eta_4) & (\eta_3+\eta_4+\eta_5) & & & \\ & & & 2\eta_5 & & \\ & & & & 2\eta_5 & \\ & & & & & 2\eta_5 \end{pmatrix}. \tag{39}$$

[Note that there are terms present in the isotropic case that do not arrive by simply taking the orientational average of (38), as we could have done – and have discussed already – for the small crack density results. The formula (39) is however obtained directly by taking the appropriate second derivatives of the elastic potential energy (59).]

And, similarly, the second order correction for the case of random vertical cracks (having normals lying randomly in horizontal planes) is:

$$\Delta S_{ij}^{(2)} = \frac{\rho_c^2}{2} \begin{pmatrix} (\eta_3+\eta_4+\eta_5) & (\eta_3+\eta_4) & \eta_4/2 & & & \\ (\eta_3+\eta_4) & (\eta_3+\eta_4+\eta_5) & \eta_4/2 & & & \\ \eta_4/2 & \eta_4/2 & 0 & & & \\ & & & \eta_5 & & \\ & & & & \eta_5 & \\ & & & & & 2\eta_5 \end{pmatrix}. \tag{40}$$

[Note: Again this result does not follow immediately from the result (38), but requires the careful use of the (61).] This case is the same one illustrated in Figure 1, but we are assuming now that $0.1 \leq \rho_c \leq 0.2$ as in the simulation data used for the fits in Berryman & Grechka (2006).

Using the same notation and the same order of approximation [*i.e.*, retaining $O(\rho_c^2)$], the Reuss averages for the bulk modulus and shear modulus of an overall isotropic system of fractures in an elastic medium with host moduli K_0 and G_0 are:

$$\frac{1}{K_R} = \frac{1}{K_0} + 2\rho_c \left[\eta_2 + \rho_c(\eta_3 + \eta_5) + 3(\eta_1 + \rho_c \eta_4)\right] \tag{41}$$

and

$$\frac{1}{G_R} = \frac{1}{G_0} + \frac{4\rho_c}{3} \left[\eta_2 + \rho_c(\eta_5 + 2\eta_3/5)\right]. \tag{42}$$

Berryman & Grechka (2006) found that the noninteraction approximation is quite accurate for the shear modulus determined by using simulation data of Grechka & Kachanov (2006a,b,c) in the random polycrystals of cracked-grains model. This means the terms of order ρ_c^2 in (42) are negligible and, therefore, also suggests that $\eta_3 \simeq -\frac{5}{2}\eta_5$.

TABLE 2 shows the results of fitting to the computer-based empirical results of Grechka and Kachanov (2006a,b,c) (from 79 simulations for $\nu_0 = 0.0000$ and another 73 simulations for $\nu_0 = 0.4375$). For both Poisson ratio values considered, the parameter combination $\eta_5 + 2\eta_3/5$ [see Eq. (42)] was found to be quite small, *e.g.*, $\eta_5 + 2\eta_3/5 \simeq 0.02$ for $\nu_0 = 0.0000$ and $\simeq 0.00$ for $\nu_0 = 0.4375$. This result suggests that setting $\eta_3 \simeq -5\eta_5/2$ may be appropriate over the full range of ν_0 normally considered pertinent to geophysics, *i.e.*, $0.0 \leq \nu_0 \leq 0.5$. Combining this observation with the further obsrevations that $\eta_1 \simeq 0.0$ and $\eta_4 \simeq 0.0$ shows that the second order correction matrices are much simpler than might have been anticipated. The main conclusion appears to be that effective isotropic shear modulus of these cracked systems at moderate crack densities does not depend in any significant way on the higher order corrections, which shows from (42) that the parameter combination $\eta_5 + 2\eta_3/5$ should vanish. We therefore use this empirical relationship to eliminate η_3 by substituting $-5\eta_5/2$ everywhere in its place.

Since we are now neglecting η_1 — as it is about two orders of magnitude smaller than the terms retained — resulting corrections contain only three combinations of the remaining parameters: $D_1 \equiv \eta_2 + \rho_c(\eta_3 + \eta_5) \simeq \eta_2 - \frac{3}{2}\rho_c\eta_5$, $D_2 \equiv \eta_2 + \rho_c\eta_5$, and $N = D_1 - D_2 = \rho_c\eta_3 \simeq -\frac{5}{2}\rho_c\eta_5$. Then, for horizontal fractures, we have

$$\Delta S_{ij}^{(1)} + \Delta S_{ij}^{(2)} \simeq \rho_c \begin{pmatrix} 0 & 0 & 0 & & & & \\ 0 & 0 & 0 & & & & \\ 0 & 0 & 2D_1 & & & & \\ & & & 2D_2 & & & \\ & & & & 2D_2 & & \\ & & & & & 0 & \end{pmatrix}. \tag{43}$$

Similarly, for the isotropic case, we have:

$$\Delta S_{ij}^{(1)} + \Delta S_{ij}^{(2)} \simeq \frac{2\rho_c}{3} \begin{pmatrix} D_1 & N & N & & & & \\ N & D_1 & N & & & & \\ N & N & D_1 & & & & \\ & & & 2D_2 & & & \\ & & & & 2D_2 & & \\ & & & & & 2D_2 & \end{pmatrix}, \tag{44}$$

while, for vertical fractures, we also have:

$$\Delta S_{ij}^{(1)} + \Delta S_{ij}^{(2)} \simeq \rho_c \begin{pmatrix} D_1 & N & 0 & & & & \\ N & D_1 & 0 & & & & \\ 0 & 0 & 0 & & & & \\ & & & D_2 & & & \\ & & & & D_2 & & \\ & & & & & 2D_2 & \end{pmatrix}. \tag{45}$$

These results differ somewhat from the corresponding results of Sayers & Kachanov (1995) and Schoenberg & Sayers (1995). For example, $D_1 \neq D_2$ in formula (43). Nevertheless, equations (44) and (45) are both valid VTI compliance correction matrices, since $2(D_1 - N) = 2D_2$. [Eq. (43) is also a valid VTI compliance correction, but trivially so since all the terms that need to be checked vanish identically.] When the crack density is sufficiently small, the results of Sayers & Kachanov (1995) and Schoenberg & Sayers (1995) will clearly be recovered. But, for higher crack densities, we expect to see some predictable deviations. The difference is due to the presence of the higher order term η_5 and the factor of crack density ρ_c.

Horizontal cracks

From (43) horizontal cracks, direct calculation shows that the main two Thomsen parameters for this problem are:

$$\gamma_h = \rho_c G_0 D_2 \tag{46}$$

and, similarly,

$$\epsilon_h = \frac{2\rho_c G_0}{1 - \nu_0} D_1. \tag{47}$$

The corresponding Reuss averages of the bulk and shear moduli are:

$$\frac{1}{K_R^h} = \frac{1}{K_0} + 2\rho_c D_1 \tag{48}$$

and, similarly,

$$\frac{1}{G_R^h} = \frac{1}{G_0} + \frac{4\rho_c}{5}\left(\frac{2}{3}D_1 + D_2\right). \tag{49}$$

Vertical cracks

From (45) for vertical cracks, direct calculation shows that the main two Thomsen parameters for this problem are:

$$\gamma_v = -\frac{1}{2}\left(\frac{\rho_c G_0 D_2}{1+2\rho_c G_0 D_2}\right) \tag{50}$$

and, similarly,

$$\epsilon_v = -\frac{\rho_c G_0}{1-\nu_0}\left(\frac{(D_1+2\nu_0 N)+\rho_c E_0(D_1^2-N^2)}{1+\frac{2\rho_c G_0}{1-\nu_0}\left[2(D_1+\nu_0 N)+\rho_c E_0(D_1^2-N^2)\right]}\right). \tag{51}$$

The corresponding Reuss averages of the bulk and shear moduli are:

$$\frac{1}{K_R^v} = \frac{1}{K_0} + 2\rho_c(D_1+N) = \frac{1}{K_0} + 2\rho_c\left(\eta_2 - 4\rho_c\eta_5\right) \tag{52}$$

and, similarly,

$$\frac{1}{G_R^v} = \frac{1}{G_0} + \frac{2\rho_c}{15}\left[(D_1+N)+9D_2\right] = \frac{1}{G_0} + \frac{2\rho_c}{3}\left(2\eta_2+\rho_c\eta_5\right). \tag{53}$$

It is straightforward to check in both cases (horizontal and vertical cracks) that the high crack density results reduce to the previously quoted low crack density results when ρ_c is small.

5.2 Examples

Expressions for phase velocities in Thomsen's weak anisotropy limit can be found many places, including Thomsen (1986) and Rüger (2002). The pertinent expressions for phase velocities as a function of angle θ, measured from the vertical direction, are

$$v_p(\theta) = v_p(0)\left(1+\delta\sin^2\theta\cos^2\theta+\epsilon\sin^4\theta\right), \tag{54}$$

$$v_{sv}(\theta) = v_s(0)\left(1+[v_p^2(0)/v_s^2(0)](\epsilon-\delta)\sin^2\theta\cos^2\theta\right), \tag{55}$$

and

$$v_{sh}(\theta) = v_s(0)\left(1 + \gamma \sin^2\theta\right). \tag{56}$$

In our present context, $v_s(0) = \sqrt{c_{44}/\rho_0}$, and $v_p(0) = \sqrt{c_{33}/\rho_0}$, where c_{33}, c_{44}, and ρ_0 are two stiffnesses of the cracked medium and the mass density of the isotropic host elastic medium. We assume that the cracks have insufficient volume to affect the mass density significantly.

We have found that in the cases studied there is a further simplification, which is apparently due to the fact that all cases considered here have either isotropic or VTI symmetry. In particular, we have found by direct computations that $\delta = \epsilon$ for low crack density materials. This result shows that $v_{sv}(\theta) \simeq v_{sv}(0)$ is approximately constant, and therefore is not very interesting. The result $\delta = \epsilon$ does not affect $v_{sh}(\theta)$, but the remaining phase velocity now reduces in the same limit to

$$v_p(\theta) = v_p(0)\left(1 + \epsilon \sin^2\theta\right). \tag{57}$$

Although some approximations (like expanding square roots) have been made to arrive at these formulas, it is still reasonable to refer to the results as having "elliptical" symmetry. By comparison, an isotropic medium has "spherical" symmetry, as the wave fronts move away from a point source at the same rate in all spatial directions.

Figures 4 and 5 show results for horizontal and vertical cracked materials for the examples having $\nu_0 = 0.00$ and $\nu_0 = 0.4375$ considered by Berryman and Grechka (2006). Recall that Thomsen's weak anisotropy approximation (Thomsen, 1986) as embodied in (54)–(56) assumes that $|\delta| \leq 0.2$, $|\epsilon| \leq 0.2$, $|\gamma| \leq 0.2$ and is designed to be most accurate at small angles from the vertical (as it is needed to be for use in reflection seismology), so the results plotted should not be taken too literally as $\theta \to 90^o$.

Exact velocities (see Appendix C) for the same values of the c_{ij}'s were plotted in black

in Figures 4 & 5, while Thomsen's approximate velocities were subsequently plotted in red. Results show that Thomsen's approximations are very close to the exact velocities for v_p out to $\theta \simeq 30^o$ or 40^o. Overall changes in both v_{sv} and v_{sh} with angle θ are small in these examples, so Thomsen's and the exact formulas agree well over the entire range of angles. Note that the peak value of v_{sv} in Thomsen's approximation always occurs at $\theta = 45^o$, whereas the true peak depends on the ratio $(c_{33} - c_{44})/(c_{11} - c_{44})$, and may be approximated by the formula $\tan^2\theta \simeq (c_{33} - c_{44})/(c_{11} - c_{44})$.

6 DISCUSSION AND CONCLUSIONS

Sayers & Kachanov (1991) introduced a convenient method of analyzing fractured (but otherwise) elastic systems. We have seen here that their method can be successfully generalized to fluid-saturated fractures. One rigorous and important result, demonstrated for low crack densities, is that the crack-influence parameters are changed under undrained conditions from $\eta_1(0)$ and $\eta_2(0)$ to $\eta_1(0)(1-B)$ and $\eta_2(0)(1-B)$, respectively, where B is Skempton's coefficient. Since B ranges from $B \simeq 0$ for vacuum or air (or fully drained conditions) and $B \to 1$ for $K_f \to K_m$, we cover the entire range of normal possibilities by inconporating this one additional parameter into the model. This result can also be generalized for higher crack densities, but discussion of this effort has been left to future work.

Furthermore, when the Sayers & Kachanov (1991) method is used in conjunction with Thomsen's anisotropy parameter (Thomsen, 1986), we find not only analytical results that aid our intuition about these complex problems, but also a means to deconstruct velocity data and then to interpret the nature (approximate crack density) of fractures in the system being studied. The magnitudes of the fracture parameters η_1 and η_2 can be determined in a straightforward way using any effective medium theory we trust (Kachanov, 1994; Prat and

Ba$\tilde{z}$ant, 1997; Grechka, 2005). And furthermore, this side calculation can be done just for the isotropic (and, therefore, the simplest) case for randomly oriented cracks. For examples of the results for penny-shaped cracks in quartz, see TABLE 1. These parameter values do not change for fixed crack shapes and fixed host medium. Only the crack density parameter ρ_c and the crack orientation distributions (for the anisotropic situations) will change. It would also be interesting and important to understand how these effects might depend on the host medium properties when the host itself is inherently anisotropic (Lyakhovitsky, 1993).

For very dilute fracture systems, any of the standard effective medium theories will actually produce virtually the same values of the parameters η_1 and η_2. The only variable is the crack shape, which was assumed here (as is most commonly done) to be penny-shaped cracks with small aspect ratios. Values of η_1 and η_2 can vary with changes in the assumed microstructure (*i.e.*, other choices of crack shapes), but values could be tabulated once and for all for the low density limit with any choices of crack shape we might ever want to consider and then the numbers would be universally available. Users would not need to be experts in effective medium theory to make use of these results — although they would, of course, still need to experts in the interpretation of seismic data and, in particular, of the Thomsen parameters themselves.

ACKNOWLEDGMENTS

The author thanks V. Grechka, M. Kachanov, S. R. Pride, and M. Schoenberg for helpful collaborations and conversations. Work performed under the auspices of the U.S. Department of Energy by the University of California, Lawrence Berkeley National Laboratory under Contract No. DE-AC03-76SF00098 and supported specifically by the Geosciences Research Program of the DOE Office of Basic Energy Sciences, Division of Chemical Sciences,

Geosciences and Biosciences.

REFERENCES

Al-Husseini, M. I., Glover, J. B., & Barley, B. J., 1981. Dispersion patterns of the ground-roll in eastern Saudi Arabia, *Geophysics*, **46** (2), 121–137 (1981).

Bažant, Z. P, & Planas, J., 1998, *Fracture and Size Effect in Concrete and Other Quasibrittle Materials*, CRC Press, New York, pp. 560–563.

Berge, P. A., Mallick, S., Fryer, G. J., Barstow, N., Carter, J. A., Sutton, G. H., & Ewing, J. I., 1991. *In situ* measurement of transverse isotropy in shallow-water marine sediments, *Geophys. J. Int.*, **104**, 241–254.

Berge, P. A., Berryman, J. G., & Bonner, B. P., 1993. Influence of microstructure on rock elastic properties, *Geophys. Res. Lett.*, **20**, 2619–2622.

Berge, P. A., Bonner, B. P, & Berryman, J. G., 1995. Ultrasonic velocity-porosity relationships for sandstone analogs made from fused glass beads, *Geophysics*, **60**, 108–119.

Berryman, J. G., 1979. Long-wave elastic anisotropy in transversely isotropic media, *Geophysics*, **44**, 896–917.

Berryman, J. G., 1980. Long-wavelength propagation in composite elastic media II. Ellipsoidal inclusions, *J. Acoust. Soc. Am.*, **68**, 1820–1831.

Berryman, J. G., 1995. Mixture theories for rock properties, in *American Geophysical Union Handbook of Physical Constants*, edited by T. J. Ahrens, AGU, New York, pp. 205–228.

Berryman, J. G., 1999. Origin of Gassmann's equations, *Geophysics*, **64**, 1627–1629.

Berryman, J. G., 2000. Seismic velocity decrement ratios for regions of partial melt in the lower mantle, *Geophys. Res. Lett.*, **27**, 421–424.

Berryman, J. G., 2004a. Modeling high-frequency acoustic velocities in patchy and partially saturated porous rock using differential effective medium theory, *Int. J. Multiscale Computational Engineering*, **2** (1), 115–131.

Berryman, J. G., 2004b. Poroelastic shear modulus dependence on pore-fluid properties arising in a model of thin isotropic layers, *Geophys. J. Int.*, **127**, 415–425.

Berryman, J. G., 2006. Estimates and rigorous bounds on pore-fluid enhanced shear modulus in poroelastic media with hard and soft anisotropy, *Int. J. Damage Mech.*, **15**, 133–167.

Berryman, J. G., & Grechka, V., 2006. Random polycrystals of grains containing cracks: Model of quasistatic elastic behavior for fractured systems, *J. Appl. Phys.*, **100**, 113527.

Berryman, J. G., & Pride, S. R., 2002. Models for computing geomechanical constants of double-porosity materials from the constituents properties, *J. Geophys. Res.*, **107**(B3), 10.1029/2000JB000108.

Berryman, J. G., Pride, S. R., & Wang, H. F., 2002. A differential scheme for elastic properties of rocks with dry or saturated cracks, *Geophys. J. Int.*, **151** (2), 597–611.

Berryman, J. G., Thigpen, L. & Chin, R. C. Y., 1988. Bulk elastic wave propagation in partially saturated porous solids, *J. Acoust. Soc. Am.*, **84**, 360–373.

Berryman, J. G., & Wang, H. F., 2000. Elastic wave propagation and attenuation in a double-porosity dual-permeability medium, in *Proceedings of the Neville G. W. Cook Conference, LBNL, October 16–17, 1998*, *Int. J. Rock Mech.*, **37**, 67–78.

Biot, M. A., 1956a. Theory of propagation of elastic waves in a fluid-saturated porous solid. I. Low-frequency range, *J. Acoust. Soc. Am.*, **28**, 168–178.

Biot, M. A., 1956b. Theory of propagation of elastic waves in a fluid-saturated porous solid. II. Higher frequency range, *J. Acoust. Soc. Am.*, **28**, 179–191.

Biot, M. A., 1962. Mechanics of deformation and acoustic propagation in porous media, *J. Appl. Phys.*, **33**, 1482–1498.

Biot, M. A., & Willis, D. G., 1957. The elastic coefficients of the theory of consolidation, *J. App. Mech.*, **24**, 594–601.

Bonner, B. P., 1974, Shear wave birefringence in dilating granite, *Geophys. Res. Lett.*, **1**, 217–220.

Brown, R. J. S., & Korringa, J., 1975. On the dependence of the elastic properties of a porous rock on the compressibility of a pore fluid, *Geophysics*, **40**, 608–616.

Bruner, W. M., 1976. Comment on "Seismic velocities in dry and saturated cracked solids" by B. Budiansky & R. J. O'Connell, *J. Geophys. Res.*, **81**, 2573–2576.

Bucher, H. P., Whitney, J. A., & Keir, D. L., 1964. Use of Stoneley waves to determine the shear wave velocity in ocean sediments, *J. Acoust. Soc. Am.*, **36**, 1595–1596.

Budiansky, B., & O'Connell, R. J., 1976. Elastic moduli of a cracked solid, *Int. J. Solids Struc.*, **12**, 81–97.

Crampin, S., 1989. Suggestions for a consistent terminology for seismic anisotropy, *Geophys. Prospecting*, **37**, 753–770.

Dvorkin, J., & Nur, A., 1998. Acoustic signatures of patchy saturation, *Int. J. Solids Struct.*, **35**, 4803–4810 (1998).

Endres, A. L., & Knight, R., 1989. The effect of microscopic fluid distribution on elastic wave velocities, *Log Anal.*, **30**, 437–444.

Ewing, W. M., Jardetsky, W. S., & Press, F., 1957. *Elastic Waves in Layered Media*, McGraw-Hill, New York.

Gassmann, F., 1951. Über die elastizität poröser medien, *Veirteljahrsschrift der Naturforschenden Gesellschaft in Zürich*, **96**, 1–23.

Grechka, V., 2005. Penny-shaped fractures revisited, *Stud. Geophys. Geod.*, **49**, 365–381.

Grechka, V., & Kachanov, M. 2006a. Effective elasticity of fractured rocks, *The Leading Edge*, **25**, 152–155.

Grechka, V., & Kachanov, M., 2006b. Effective elasticity of rocks with closely spaced and intersecting cracks, *Geophysics*, **71**, D85–D91 (2006).

Grechka, V., & Kachanov, M., 2006c. Seismic characterization of multiple fracture sets: Does orthotropy suffice?, *Geophysics*, **71**, D93–D105.

Hashin, Z., & Shtrikman, S., 1963. A variational approach to the theory of the elastic behaviour of multiphase materials, *J. Mech. Phys. Solids*, **11**, 127–140.

Henyey, F. S., & Pomphrey, N., 1982. Self-consistent elastic moduli of a cracked solid, *Geophys. Res. Lett.*, **9** (8), 903–906.

Hildebrand, F. B., 1956. *Introduction to Numerical Analysis*, Dover Publications, New York, pp. 575–578.

Hornby, B. E., 1994. *The Elastic Properties of Shales*, Ph.D. dissertation, University of Cambridge, Cambridge, UK.

Hudson, J. A., 1980. Wave speeds and attenuation of elastic waves in material containing cracks, *Geophys. J. R. Astron. Soc.*, **64**, 133–150.

Hudson, J. A., 1986. A higher order approximation to the wave propagation constants for a cracked solid, *Geophys. J. R. Astron. Soc.*, **87**, 265–274.

Hudson, J. A., 1994. Overall properties of a material with inclusions or cavities, *Geophys. J. Int.*, **117**, 555–561.

Ji, C., Tsuboi, S., Komatitsch, D., & Tromp, J., 2005. Rayleigh-wave multipathing along the west coast of North America, *Bull. Seismol. Soc. Am.*, **95** (6), 2115–2124.

Johnson, D. L., 2001. Theory of frequency dependent acoustics in patchy-saturated porous media, *J. Acoust. Soc. Am.*, **110**, 682–694.

Jones, R., 1958. *In situ* measurement of the dynamic properties of soil by vibration methods, *Geotechnique*, **8**, 1–21.

Kachanov, M., 1980. Continuum model of medium with cracks, *ASCE J. Engineering Mech.*, **106**, 1039–1051.

Kachanov, M., 1994. Elastic solids with many cracks and related problems, in *Advances in Applied Mechanics*, edited by J. W. Hutchinson and T. Y. Wu, Academic Press, Boston, Massachusetts, pp. 260–445.

Keller, J. B., 1964. Stochastic equations and wave propagation in random media, *Proc. Symp. appl. Math.*, **16**, 145–170.

Love, A. E. H., 1927. *A Treatise on the Mathematical Theory of Elasticity*, Dover, New York, pp. 307–309.

Lyakhovitsky, F. M., 1993. Velocity of P-waves in transversely isotropic media, *Canadian J. Explor. Geophys.*, **29**, 114–116.

Lynn, H. B., Simon, K. M., Layman, M., Schneider, R., Bates, C. R., & Jones, M., 1995. Use of anisotropy in P-wave and S-wave data for fracture characterization in a naturally fractured gas reservoir, *The Leading Edge*, **14**, 887–893.

Mavko, G., & Jizba, D., 1991. Estimating grain-scale fluid effects on velocity dispersion in rocks, *Geophysics*, **56**, 1940–1949.

Mavko, G., & Nolen-Hoeksema, R., 1994. Estimating seismic velocities at ultrasonic frequencies in partially saturated rocks, *Geophysics*, **59**, 252–258.

Murphy, W. F., III, 1982. *Effects of Microstructure and Pore Fluids on the Acoustic Properties of Granular Sedimentary Materials*, Ph.D. Dissertation, Stanford University, Stanford, CA.

Murphy, W. F., III, 1984. Acoustic measures of partial gas saturation in tight sandstones, *J. Geophys. Res.*, **89**, 11549–11559.

Musgrave, M. J. P., 1959. The propagation of elastic waves in crystals and other anisotropic media, *Reports Prog. Phys.*, **22**, 74–96.

O'Connell, R. J., & Budiansky, B., 1974. Seismic velocities in dry and saturated cracked solids, *J. Geophys. Res.*, **79**, 5412–5426.

O'Connell, R. J., & Budiansky, B., 1977. Viscoelastic properties of fluid-saturated cracked solids, *J. Geophys. Res.*, **82**, 5719–5736.

Prat, P. C., & Ba$\tilde{z}$ant, Z. P., 1997. Tangential stiffness of elastic materials with systems of growing or closing cracks, *J. Mech. Phys. Solids*, **45**, 611–636.

Press, W. H., Flannery, B. P., Teukolsky, S. A., & Vetterling, W. T., 1988. *Numerical Recipes in C: The Art of Scientific Computing*, Cambridge University Press, New York, pp. 270–275.

Pride, S. R., 2005. Relationships between seismic and hydrological properties, in *Hydrogeophysics*, edited by Y. Rubin & S. Hubbard, Springer, New York, pp. 253–291.

Pride, S. R., & Berryman, J. G., 2003a. Linear dynamics of double-porosity dual-permeability materials I. Governing equations and acoustic attenuation, *Phys. Rev. E*, **68**, 036603 (September 9, 2003).

Pride, S. R., & Berryman, J. G., 2003b. Linear dynamics of double-porosity dual-permeability materials II. Fluid transport equations, *Phys. Rev. E*, **68**, 036604 (September 9, 2003).

Pride, S. R., Berryman, J. G., & Harris, J. M., 2004. Seismic attenuation due to wave-induced flow, *J. Geophys. Res.*, **109**, B01201 (January 14, 2004).

Pride, S. R., Harris, J. M., *et al.*, 2003. Permeability dependence of seismic amplitudes, *The Leading Edge*, **22**, 518–525.

Rathore, J. S., Fjaer, E., Holt, R. M., & L. Renlie, L., 1995. Acoustic anisotropy of a synthetic sanstone with controlled crack geometry, *Geophys. Prosp.* **43**, 711–728.

Rüger, A., 1998. Variation of P-wave reflectivity with offset and azimuth in anisotropic media, *Geophysics*, **63**, 935–947.

Rüger, A., 2002, *Reflection Coefficients and Azimuthal AVO Analysis in Anisotropic Media*, Geophysical Monographs Series, Number 10, SEG, Tulsa, OK.

Sayers, C. M., 1988. Inversion of ultrasonic wave velocity measurements to obtain microcrack orientation distribution function in rocks, *Ultrasonics*, **26**, 73–77.

Sayers, C. M., & Kachanov, M., 1991. A simple technica for finding effective elastic constants of cracked solids for arbitrary crack orientation statistics," *Int. J. Solids Struct.*, **27**, 671–680.

Sayers, C. M., & Kachanov, M., 1995. Microcrack-induced elastic wave anisotropy of brittle rocks, *J. Geophys. Res.*, **100**, 4149–4156.

Schoenberg, M., & Sayers, C. M., 1995. Seismic anisotropy of fractured rock, *Geophysics*, **60**, 204–211.

Skempton, A. W., 1954. The pore-pressure coefficients A and B, *Géotechnique*, **4**, 143–147.

Thomsen, L., 1986. "Weak elastic anisotropy, *Geophysics*, **51**, 1954–1966.

Thomsen, L., 1995. Elastic anisotropy due to aligned cracks in porous media, *Geophys. Prosp.*, **43**, 805–829.

Thomsen, L., 2002. *Understanding Seismic Anisotropy in Exploration and Exploitation*, 2002 Distinguished Instructor Short Course, Number 5, SEG, Tulsa, OK.

Tod, S. R., 2002. The effects of stress and fluid pressure on the anisotropy of interconnected cracks, *Geophys. J. Int.*, **149**, 149–156.

Tod, S. R., 2003. An anisotropic fractured poroelastic effective medium theory, *Geophys. J. Int.*, **155**, 1006–1020.

Wawersik, W. R., Orr, F. M., Rudnicki, J. W., Ortoleva, P. J., Dove, P., Richter, F., Harris, J., Warpinski, N. R., Logan, J. M., Wilson, J. L., Pyrak-Nolte, L., & Wong, T.-F., 2001, Terrestrial sequestration of CO_2: An assessment of research needs, *Advances in Geophysics*, **43**, 97–177.

Weertman, J., 1996. *Dislocation-Based Fracture Mechanics*, World Scientific, River Edge, NJ.

Winterstein, D. F., 1990. Velocity anisotropy terminology for geophysicists, *Geophysics*, **55**, 1070–1088.

Zimmerman, R. W., 1991. *Compressibility of Sandstones*, Elsevier, Amsterdam.

Appendix A: Crack-influence Decomposition Method

Sayers & Kachanov (1991) present a useful method for decomposing the elastic potential of a cracked system into parts due to the (assumed) homogeneous and isotropic elastic background material, and those due to the presence of cracks up to moderate crack densities ($\rho_c \simeq 0.1$). The fundamental idea is that the elastic potential function is composed of just nine terms, representing all combinations of stress invariants of such a system. These invariants depend on the stress tensor σ and the crack density tensor α. In particular, the tensor α is defined in three dimensions by

$$\alpha = \frac{1}{V} \sum_c a_c^3 \hat{n}_c \hat{n}_c^T, \tag{58}$$

where V is the averaging volume, $\hat{n}_c$ is the unit normal of penny-shaped crack c having radius a_c. We use the notation $\hat{n}_c \hat{n}_c^T$, where T is the transpose, to express the outer product $(\hat{n}_c \otimes \hat{n}_c)$ of two vectors; this notation is consistent with that commonly used to express the singular value decomposition of an arbitrary matrix in terms of its singular vectors. Another common, and entirely equivalent, form of notation for the same quantity that is often used in the mechanics literature is the dyadic form $\boldsymbol{n}_c \boldsymbol{n}_c$.

The elastic potential $\Phi(\sigma, \alpha)$ then takes the form

$$\begin{aligned} \Phi(\sigma,\alpha) = {} & \Phi_1^{(0)}[\mathrm{Tr}(\sigma)]^2 + \Phi_2^{(0)}\mathrm{Tr}(\sigma\cdot\sigma) + \eta_1\mathrm{Tr}(\sigma)\mathrm{Tr}(\sigma\cdot\alpha) \quad + \eta_2\mathrm{Tr}(\sigma\cdot\sigma\cdot\alpha) \\ & + \eta_3[\mathrm{Tr}(\sigma\cdot\alpha)]^2 \quad + \eta_4\mathrm{Tr}(\sigma)\mathrm{Tr}(\sigma\cdot\alpha\cdot\alpha) + \eta_5\mathrm{Tr}(\sigma\cdot\sigma\cdot\alpha\cdot\alpha) \\ & + \eta_6\mathrm{Tr}(\sigma\cdot\alpha)\mathrm{Tr}(\sigma\cdot\alpha\cdot\alpha) \quad + \eta_7[\mathrm{Tr}(\sigma\cdot\alpha\cdot\alpha)]^2, \end{aligned} \tag{59}$$

where Tr is the trace operation, and the dot notation indicates a contraction over one set of indices. (Note that the significance of coefficients η_4, η_6, and η_7 have been changed here from the definitions made by Kachanov (1980), Kachanov and Sevostianov (2005), and Sayers and Kachanov (1991), so that here η_4 is the coefficient of a contribution second order in α,

η_6 third order in α, and η_7 fourth order in α.) The coefficients pertinent to the isotropic host elastic medium are given by $\Phi_1^{(0)} = (1+\nu_0)/2E_0$ and $\Phi_2^{(0)} = -\nu_0/2E_0$, where E_0 is Young's modulus, and ν_0 is Poisson's ratio for the host material.

Now, to illustrate the meaning of (59), we reduce this to component form in two examples. For the cases of interest, we can assume the crack density tensor itself reduces to the form

$$\alpha = \sum_{i=1}^{3} \rho_i \hat{n}_i \hat{n}_i^T, \tag{60}$$

where $\hat{n}_i$, for $i = 1, 2, 3$, correspond to spatial directions x, y, z, respectively. Furthermore, $\mathrm{Tr}(\alpha) = \rho_1 + \rho_2 + \rho_3 \equiv \rho_c = na^3$ is the scalar crack density defined in the main text.

A.1 Vertical cracks only, $\rho_c = \rho_1 + \rho_2$

Our first example is one with all vertical cracks, having their crack normals in the xy-plane. Then, $\rho_c = \rho_1 + \rho_2$. A special case of this type is when the crack normals are completely randomly distributed so that $\rho_1 = \rho_2 = \rho_c/2$. Then, we get simplified formulas for all the terms in the elastic potential. The results are:

$$\begin{aligned}\Phi(\sigma,\alpha) = \Phi_1^{(0)}[\mathrm{Tr}(\sigma)]^2 + \Phi_2^{(0)}\mathrm{Tr}(\sigma\cdot\sigma) + (\eta_1\rho_c/2 + \eta_4\rho_c^2/4)(\sigma_{11}+\sigma_{22}+\sigma_{33})(\sigma_{11}+\sigma_{22}) \\ +(\eta_2\rho_c/2 + \eta_5\rho_c^2/4)(\sigma_{1j}\sigma_{j1} + \sigma_{2j}\sigma_{j2}) + (\eta_3\rho_c^2/4 + \eta_6\rho_c^3/8 + \eta_7\rho_c^4/16)(\sigma_{11}+\sigma_{22})^2,\end{aligned} \tag{61}$$

where again the repeated index j is summed.

At low crack densities ρ_c, we see that only the terms proportional to η_1 and η_2 are important in the crack-influence decomposition. As the crack density increases, the terms proportional to η_3, η_4, and η_5 start to contribute. Then, at the highest crack densities considered, all seven of these coefficients come into play. Although we may imagine, for example, that $\eta_2(\rho_c) \simeq \eta_2(0) + \rho_c\eta_2'(0)$ is actually a function of crack density ρ_c, it is clear

from the form of (61) that the corrections $\eta_2'(0)$ will be indistinguishable (at this order of approximation) from corrections due to $\eta_5(0)$ [also assuming no other information is available concerning functional forms, etc.]. So, at low crack densities, we do not need to consider any coefficients except $\eta_1(0)$ and $\eta_2(0)$. When we need to fit quadratic corrections for the moderate crack density results, it is sufficient to consider only coefficients $\eta_1(0)$ through $\eta_5(0)$.

When the situation we are considering has only vertical cracks, then the following remarks apply (but also see the discussion in the third subsection about the mixed problem): For small to moderate crack densities ρ_c, we do not need to consider ρ_c dependence of $\eta_1(\rho_c)$ or $\eta_2(\rho_c)$, as such dependence cannot be distinguished from the low order contributions from $\eta_4(0)$ and $\eta_5(0)$, respectively. Similarly, $\eta_3(0)$ comes into play whenever $\eta_4(0)$ and $\eta_5(0)$ are important, while $\eta_6(0)$ and $\eta_7(0)$ can presumably always be neglected in most low to moderate crack density applications.

Similar remarks apply here when the only information available is from collections of horizontal cracks.

A.2 Horizontal cracks only, $\rho_c = \rho_3$

If all the cracks in the system have the same axis of symmetry (which we will take to be the vertical or z-axis), then $\rho_c = \rho_3$ and (59) reduces to the following expression:

$$\begin{aligned}\Phi(\sigma,\alpha) = \Phi_1^{(0)}[\mathrm{Tr}(\sigma)]^2 + \Phi_2^{(0)}\mathrm{Tr}(\sigma\cdot\sigma) \,+\, (\eta_1\rho_c + \eta_4\rho_c^2)(\sigma_{11}+\sigma_{22}+\sigma_{33})\sigma_{33} \\ +(\eta_2\rho_c + \eta_5\rho_c^2)\sigma_{3j}\sigma_{j3} \,+\, (\eta_3\rho_c^2 + \eta_6\rho_c^3 + \eta_7\rho_c^4)\sigma_{33}^2,\end{aligned} \tag{62}$$

where the repeated index j is summed.

Typical values of ρ_c of interest in many applications are around $\rho_c = 0.1$ (or less). So as long as the η's for higher order corrections are of approximately the same order of magni-

tude as those for $\eta_1(0)$ and $\eta_2(0)$, we see that neglect of terms like $\eta_6\rho_c^3 + \eta_7\rho_c^4$ is entirely appropriate.

Now it is also easy to see how (61) gives rise to the low density result (3), and also how (62) gives rise to (2).

A.3 Both horizontal and vertical crack information available

Results of Berryman and Grechka (2006) show that, for vertical cracks at moderate crack densities, the only higher order corrections of importance are those due to η_5. For vertical cracks, η_2 and η_5 appear together only in the combination $\eta_2\rho_c + \eta_5\rho_c^2$, whereas, for horizontal cracks, they appear together only in the combination $\eta_2\rho_c/2 + \eta_5\rho_c^2/4$. So, under these circumstances, it would be possible to distinguish the contributions of the first correction to $\eta_2 - \eta_2(0) \simeq \rho_c\eta_2'(0)$ from the contributions due only to $\eta_5(0)$, since then we could define quantities:

$$\eta_5^v(0) \equiv \eta_5(0) + \eta_2'(0) \tag{63}$$

and

$$\eta_5^h(0) \equiv \eta_5(0) + 2\eta_2'(0) \tag{64}$$

(for the vertical and horizontal cases respectively), which are clearly the values that are actually obtained in the two separate data sets. Then, we see that the values of $\eta_2'(0)$ and the true $\eta_5(0)$ are obtained by considering the two combinations

$$\eta_5^h(0) - \eta_5^v(0) = \eta_2'(0), \tag{65}$$

and

$$2\eta_5^v(0) - \eta_5^h(0) = \eta_5(0). \tag{66}$$

The paper by Berryman and Grechka (2006) made use only of numerical experiments on vertical cracks, and so was not able to separate these effects, since only $\eta_5^v(0)$ was measured. This situation can be remedied in the future by doing further simulations in order to fill in information that is currently unavailable.

Appendix B: Thomsen parameters for higher crack densities

The three Thomsen parameters (Thomsen, 1986) for weak anisotropy are $\gamma = (c_{66} - c_{44})/2c_{44}$, $\epsilon = (c_{11} - c_{33})/2c_{33}$, and

$$\delta = \frac{(c_{13} + c_{44})^2 - (c_{33} - c_{44})^2}{2c_{33}(c_{33} - c_{44})} = \left(\frac{c_{13} + c_{33}}{2c_{33}}\right)\left(\frac{c_{13} + 2c_{44} - c_{33}}{c_{33} - c_{44}}\right). \tag{67}$$

All three of these parameters can play important roles in the velocities given by (54)-56) when the crack densities are high enough. If crack densities are low, then the SV shear wave will have no dependence on angle of wave propagation. Note that the so-called anellipticity parameter $A = \epsilon - \delta$, vanishes when $\epsilon \equiv \delta$, which has been shown to happen for low crack densities.

To avoid encumbering the main text, we will collect some of the more difficult results for higher crack densities here. Recall that, for low crack densities, we have the helpful simplification that $\delta \simeq \epsilon$, so the wave speed formulas reduce to elliptical symmetry, and the expressions for the coefficients γ and ϵ themselves are also relatively simple. However, for the higher crack density results, we find that $\delta \neq \epsilon$, and, furthermore, the resulting expressions for the parameters, especially for δ, become difficult and unwieldy. We have displayed the results for the γ_h and ϵ_h of horizontally cracked systems in (46) and 47) and for γ_v and ϵ_v of vertically cracked systems in (50) and 51). We collect the results for δ_h and δ_v here.

B.1 Thomsen parameter δ_h for horizontal cracks

Note that for horizontal fractures/cracks, the ratio $\frac{c_{13}}{c_{33}} = (\nu_0 - \rho_c \eta_1 E_0)/(1-\nu_0)$. For small ρ_c we then have the factor $\frac{c_{13}+c_{33}}{2c_{33}} \simeq 1/2(1\nu_0)$ in (67).

The final result for δ_h is given by

$$\delta_h = \frac{2\rho_c G_0}{(1-\nu_0)} \left[\frac{2(1-\nu_0)D_1 - (1-2\nu_0)D_2}{1 + 2(1-\nu_0)\rho_c G_0 (D_2 - D_1)} \right]. \tag{68}$$

To check the low crack density limit, we note that $D_1 \to D_2 \to \eta_2(0)$ as $\rho_c \to 0$. So we have the limiting result

$$\delta_h \to \frac{2\rho_c \eta_2 G_0}{(1-\nu_0)} \tag{69}$$

in agreement with (37) and (47).

For the wave speeds in this case, we also need to know

$$c_{44} = \frac{G_0}{1 + 2\rho_c G_0 D_2} \tag{70}$$

and

$$c_{33} = \frac{E_0}{1 + 2\rho_c E_0 D_1 - 2\nu_0^2/(1-\nu_0)}. \tag{71}$$

B.2 Thomsen parameter δ_v for vertical cracks

The fundamental formulas for the Thomsen parameters do not change with the anisotropy medium symmetry. So Eq. (67) is again the appropriate formula for the case of vertical cracks. On the other hand, the difficulty of the analysis rises considerably in this case, and it does not seem appropriate to show details here. Rather the four terms that need to be computed in order to evaluate (67) and the wave speeds (54)–(56) will be given instead.

The pertinent shear modulus is easily computed as

$$c_{44} = \frac{G_0}{1 + \rho_c G_0 D_2}. \tag{72}$$

The remaining two components of the formula depend on the determinant of the upper 3×3 matrix of the perturbed compliance. Using (45), we find

$$Det = \frac{1}{E_0^2}\left[\frac{(1+\nu_0)^2(1-2\nu_0)}{E_0} + 2\rho_c(1+\nu_0)[(1-\nu_0)D_1 + \nu_0 N] + \rho_c^2 E_0(D_1^2 - N^2)\right]. \quad (73)$$

Then, we have

$$c_{13} = \frac{\nu_0}{E_0}\left[\frac{1+\nu_0}{E_0} + \rho_c(D_1 - N)\right]/Det, \quad (74)$$

and, finally,

$$c_{33} = \left[\frac{1-\nu_0^2}{E_0^2} + \frac{2\rho_c}{E_0}(D_1 + \nu_0 N) + \rho_c^2\left(D_1^2 - N^2\right)\right]/Det. \quad (75)$$

Evaluating these expressions numerically and then plugging the numbers into (67) produces the results seen in Figures 4 and 5. Note that, when $\nu_0 = 0.00$, we have $c_{33} = K_0 + 4G_0/3 \equiv E_0$, which explains the convergence of the results for small θ in Fig. 5a.

Appendix C: Exact seismic velocities for VTI media

Thomsen's weak anisotropy method (Thomsen, 1986), being an approximation designed specifically for use in velocity analysis for exploration geophysics, is clearly not exact. Approximations incorporated into the formulas become most apparent for greater angles θ from the vertical, especially for $v_p(\theta)$ and $v_{sv}(\theta)$.

For reference purposes, we include here the exact velocity formulas for P, SV, and SH seismic waves at all angles in a VTI elastic medium. These results are available in many places, but are taken specifically from Berryman (1979) with some minor changes of notation. The results are:

$$v_p^2(\theta) = \frac{1}{2\rho}\left\{\left[(c_{11}+c_{44})\sin^2\theta + (c_{33}+c_{44})\cos^2\theta\right] + R(\theta)\right\} \quad (76)$$

and

$$v_{sv}^2(\theta) = \frac{1}{2\rho}\left\{\left[(c_{11}+c_{44})\sin^2\theta + (c_{33}+c_{44})\cos^2\theta\right] - R(\theta)\right\}, \tag{77}$$

where

$$R(\theta) = \sqrt{\left[(c_{11}-c_{44})\sin^2\theta - (c_{33}-c_{44})\cos^2\theta\right]^2 + 4\left(c_{13}+c_{44}\right)^2\sin^2\theta\cos^2\theta} \tag{78}$$

and, finally,

$$v_{sh}^2(\theta) = \frac{1}{\rho}\left[c_{44} + (c_{66}-c_{44})\sin^2\theta\right]. \tag{79}$$

In each case, Thomsen's approximation has included a step that removes the square on the left-hand side of the equation, by (Taylor) expanding a square root of the right hand side. This step introduces a factor of $\frac{1}{2}$ multiplying the $\sin^2\theta$ terms on the right hand side, and — for example — immediately explains how equation (56) is obtained from (79). The other two equations for $v_p(\theta)$ and $v_{sv}(\theta)$, *i.e.*, (54) & (55), involve additional approximations as well that we will not attempt to explain here.

TABLE 1. Examples of Sayers & Kachanov (1991) crack-influence parameters $\eta_1(\rho_c)$ and $\eta_2(\rho_c)$, when crack density $\rho_c << 1$ for penny-shaped cracks in quartz. Four choices of effective medium theory are considered: NI (non-inteacting), DS, (differential scheme), CPA (coherent potential approximation), and SC (the Budiansky and O'Connell self-consistent scheme). Note that crack density is defined here as $\rho_c = Nr^3/V$, where N/V is number density of cracks, and $A = \pi r^2$ is the area of the circular crack face.

	η_1 (GPa^{-1})	η_2 (GPa^{-1})
NI	-0.000216	0.0287
DS	-0.000216	0.0290
CPA	-0.000258	0.0290
SC	-0.0000207	0.0290

TABLE 2. Values of five crack-influence parameters of Sayers & Kachanov (1991) for two examples of host elastic media ($\nu_0 = 0.00$ and $\nu_0 = 0.4375$) considered in the text.

S & K (1991)	*First Example*	*Second Example*
Parameter	$\nu_0 = 0.00$	$\nu_0 = 0.4375$
$\eta_1(0)$ (GPa^{-1})	0.0000	-0.0192
$\eta_2(0)$ (GPa^{-1})	0.1941	0.3994
$\eta_3(0)$ (GPa^{-1})	-0.3666	-1.3750
$\eta_4(0)$ (GPa^{-1})	0.0000	0.0000
$\eta_5(0)$ (GPa^{-1})	0.0917	0.5500

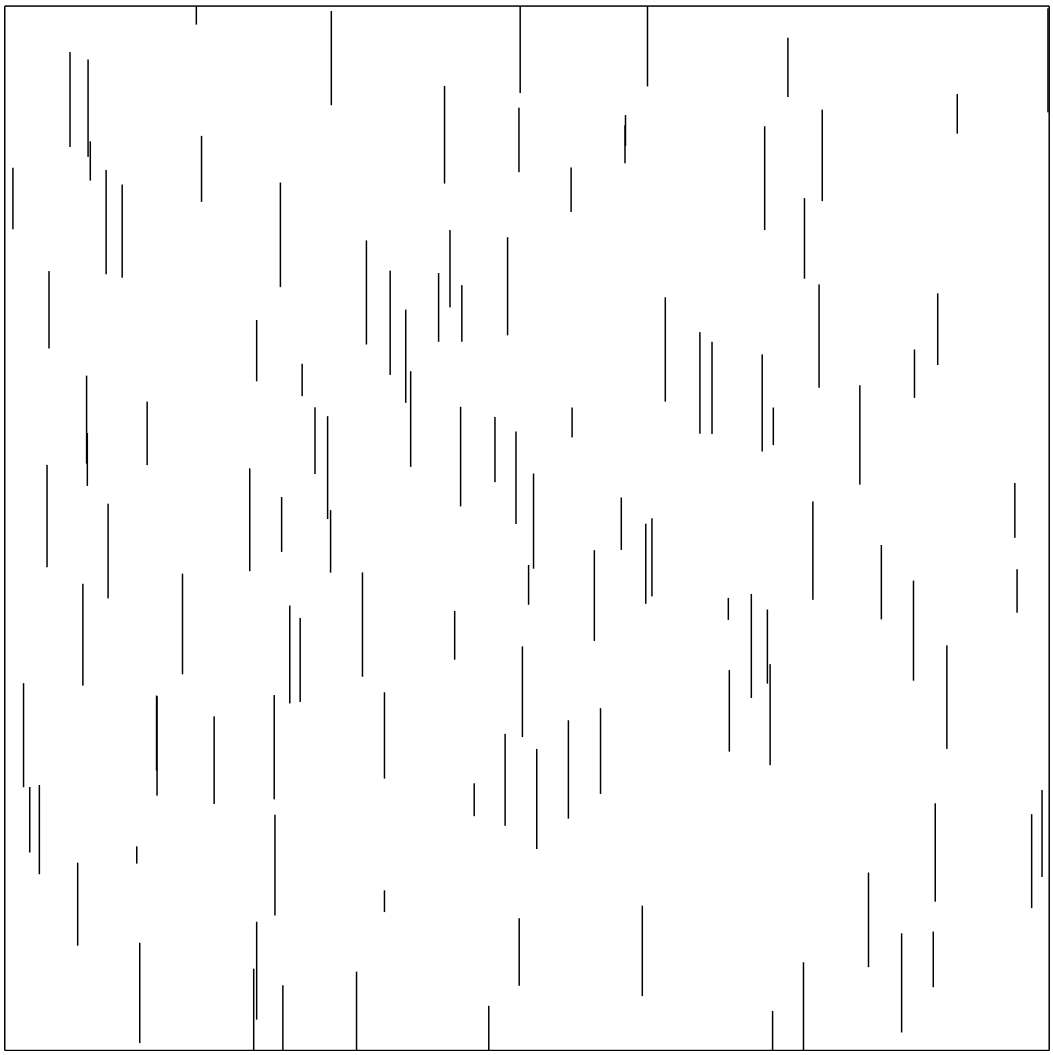

FIG. 1: Example of a vertical cross-section (xz-plane) through a medium having penny-shaped cracks with radius $r/L = 0.05$, where $L = 1.0$ is the length on each side of a cube in 3D. This image was produced by randomly placing 2000 crack centers in the box of volume $= L^3$ (so crack density $\rho_c = 0.25$), and testing to see if the center is within a distance $r \leq 0.05$ of the central square at $y = 0.5$. If so, then a random angle is chosen for the crack. If this crack orientation results in an intersection with the plane $y = 0.5$, the line of intersection is plotted here. The resulting lines can have any length from $2r = 0.1$ to zero. The number of intersections found for this realization was 114, whereas the expected value for any particular realization is approximately $(2/\pi) \times 200 \simeq 127$.

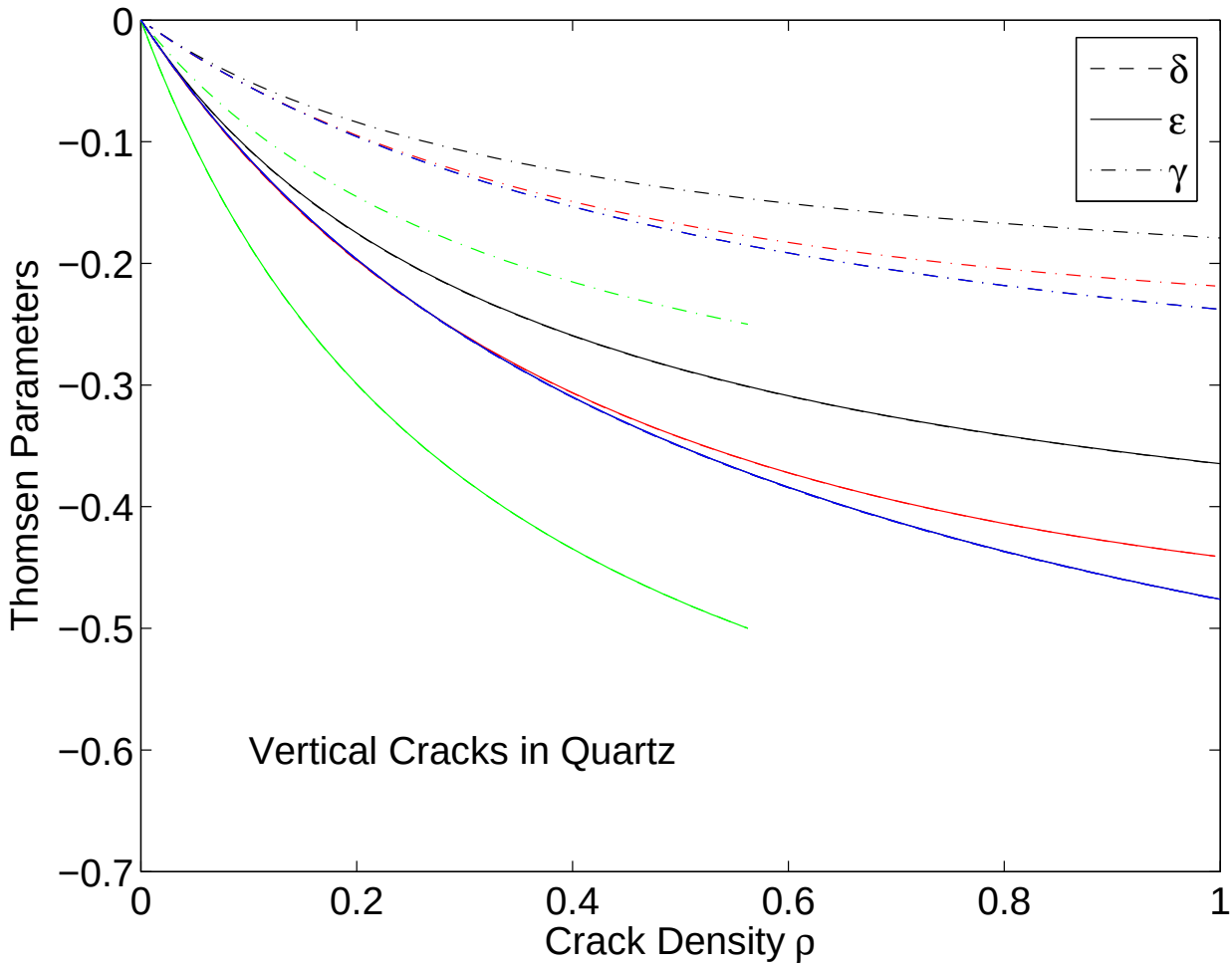

FIG. 2: Computed values of the Thomsen parameters δ, ϵ, γ, for four distinct EMT models: noninteracting (black), CPA (red), DS (blue) and the Budiansky-O'Connell self consistent (green). The parameter δ is not seen separately here because for this choice of crack microstructure (randomly oriented vertical cracks) $\delta = \epsilon$ to the order to which we are working, for small crack densities.

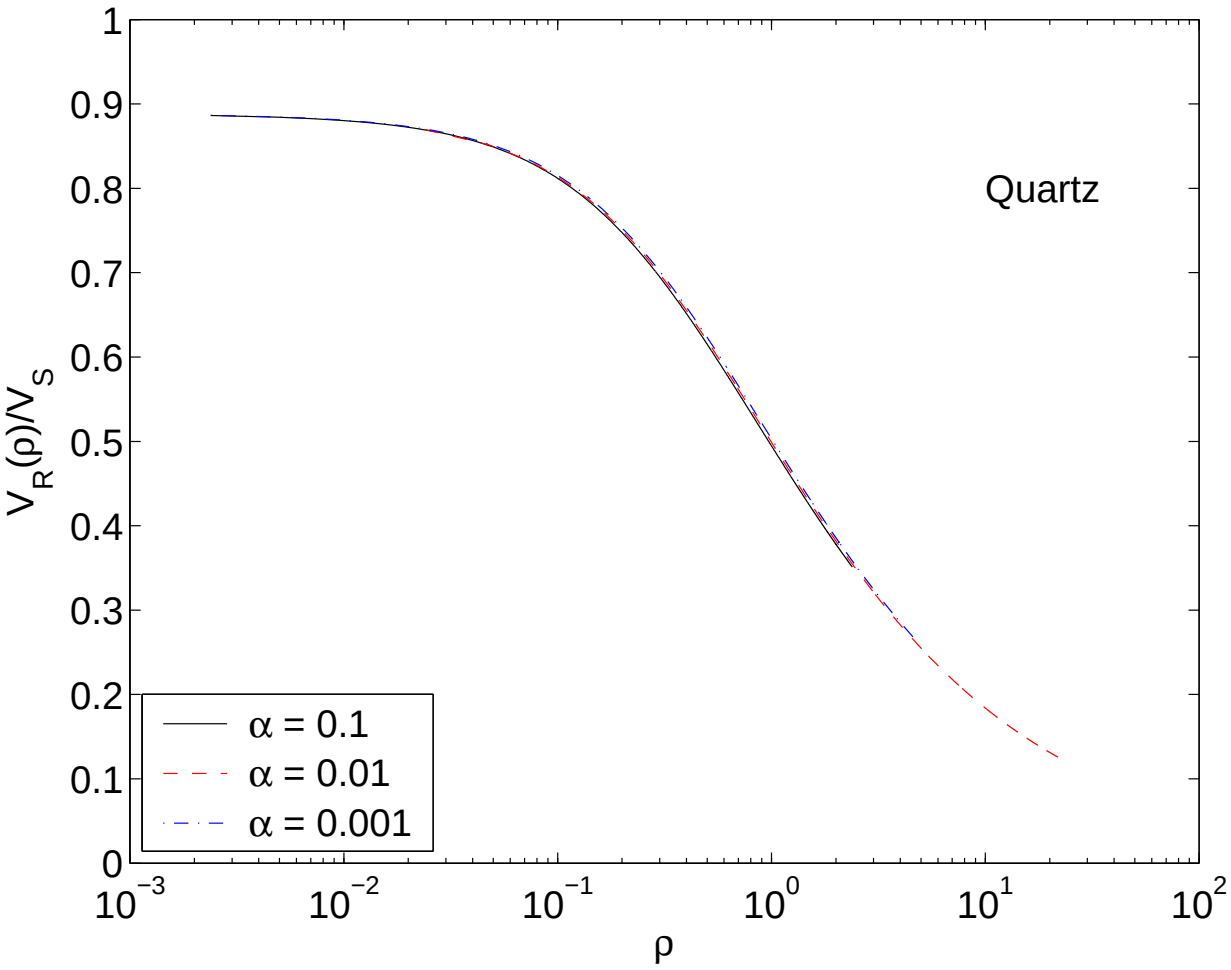

FIG. 3: Computation of Rayleigh wave speed in quartz with horizontally aligned cracks for three choices of penny-crack aspect ratio α, and a range of values of the crack density ρ_c. The assumption (prediction) is that aspect ratio α does not really matter. Only crack density ρ_c matters. So all three curves should overlap. The results show that they do overlap here at all the lower crack densities ($\rho_c \leq 0.1$).

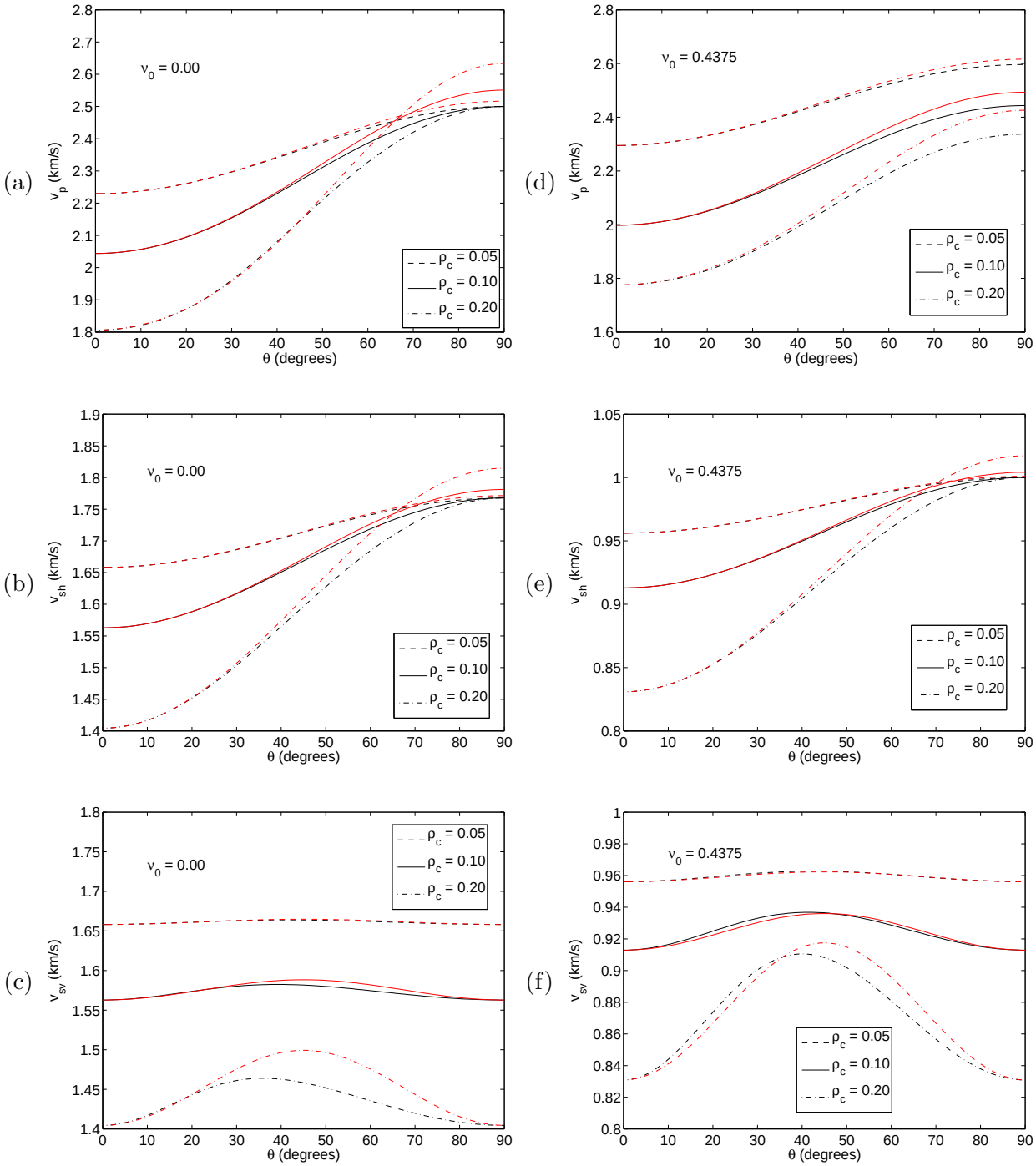

FIG. 4: For horizontal cracks: examples of anisotropic compressional wave speed (v_p), SH shear wave speed (v_{sh}), and SV shear wave speed (v_{sv}) for two values of Poisson's ratio ν_0 of the host medium: (a)–(c) $\nu_0 = 0.00$, (d)–(f) $\nu_0 = 0.4375$. Velocity curves in black are exact for the fracture model discussed in the text. The Thomsen weak anisotropy velocity curves for the same fracture model are then overlain in red.

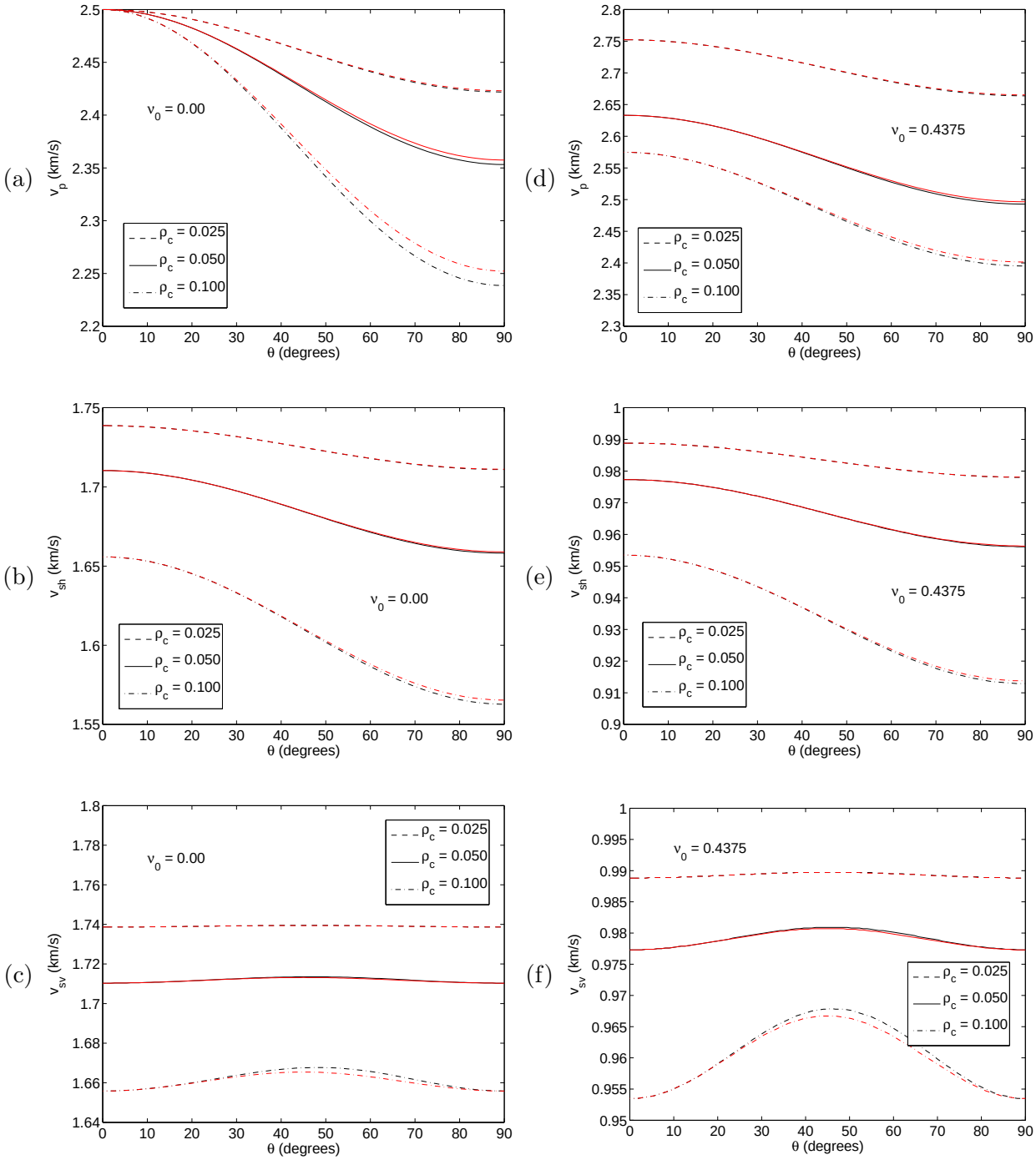

FIG. 5: For vertical cracks: examples of anisotropic compressional wave speed (v_p), SH shear wave speed (v_{sh}), and SV shear wave speed (v_{sv}) for two values of Poisson's ratio ν_0 of the host medium: (a)–(c) $\nu_0 = 0.00$, (d)–(f) $\nu_0 = 0.4375$. Velocity curves in black are exact for the fracture model discussed in the text. The Thomsen weak anisotropy velocity curves for the same fracture model are then overlain in red.